Dear Editor,

Thank you very much for your careful reading of our manuscript.
We have revised our manuscript in line with what has been exposed in the response to the reviewers. We also have accounted for your additional editorial comments as detailed below:

- We have removed the words last glacial from the first line of the abstract

- P1-L33: we have added “over Greenland” to specify the region relevant to the temperature change we highlight.

- P1-L40: we have removed the words “dissolved inorganic” as suggested

- P2-L12: we have replaced “impaired” by “biased”

- P2-L18: we have removed the inappropriate reference

- We hear the necessity to make ideas clear about the single and dual responses. We have removed the word “unique response” throughout the text and we have now used only the terminology “single” and “dual responses”, consistently with the terminology used in Figure 3.

- We have added the units (years) in Figure 4’s caption. We have removed the expression “response time” throughout the manuscript and have replaced by “time of response”.

- P9 -L14: we have replaced the word “classical” by the word “common”.

We have attached the revised manuscript as well as a tracked changes version. We sincerely hope our manuscript is now ready for publication.

All the best,

Lise Missiaen, on behalf of the author team.

Carbon isotopes and Pa/Th response to forced circulation changes: a model perspective

L. Missiaen[1,2], N. Bouttes[1], D.M. Roche[1,3], J-C. Dutay[1], A. Quiquet[1,4], C. Waelbroeck[1], S. Pichat[5,6], J-Y Peterschmitt[1]

[1]Laboratoire des Sciences du Climat et de l'Environnement, LSCE/IPSL, CEA-CNRS-UVSQ-Université Paris-Saclay, F-91198 Gif-sur-Yvette, France.
[2]Climate Change Research Centre, University of New South Wales, Sydney, Australia
[3]Vrije Universiteit Amsterdam, Faculty of Science, Cluster Earth and Climate, de Boelelaan 1085, 1081HV Amsterdam, The Netherlands
[4]Institut Louis Bachelier, Chair Energy and Prosperity, Paris, 75002, France
[5]Université de Lyon, ENS de Lyon, Laboratoire de Géologie de Lyon (LGL-TPE), F-69007 Lyon, France.
[6]Climate Geochemistry Department, Max Planck Institute for Chemistry, Mainz, Germany.

Correspondence to: Lise Missiaen (l.missiaen@unsw.edu.au)

Abstract. Understanding the ocean circulation changes associated with abrupt climate events is key to better assess climate variability and understand its different natural modes. Sedimentary Pa/Th, benthic $\delta^{13}C$ and $\Delta^{14}C$ are common proxies used to reconstruct past circulation flow rate and ventilation. To overcome the limitations of each proxy taken separately, a better approach is to produce multi-proxy measurements on a single sediment core. Yet, different proxies can provide conflicting information about past ocean circulation. Thus, modelling them in a consistent physical framework has become necessary to assess the geographical pattern, the timing and sequence of the multi-proxy response to abrupt circulation changes.

We have implemented a representation of the ^{231}Pa and ^{230}Th tracers into the model of intermediate complexity iLOVECLIM, which already included $\delta^{13}C$ and $\Delta^{14}C$. We have further evaluated the response of these three ocean circulation proxies to a classical abrupt circulation reduction obtained by freshwater addition in the Nordic seas under preindustrial boundary conditions. Without an a priori guess, the proxy response is shown to cluster in modes that resemble the modern Atlantic water masses. The clearest and most coherent response is obtained in the deep (> 2,000m) Northwest Atlantic, where $\delta^{13}C$ and $\Delta^{14}C$ significantly decrease while Pa/Th increases. This is consistent with observational data across millennial scale events of the last glacial. Interestingly, while in marine records, except in rare instances, the phase relationship between these proxies remains unclear due to large dating uncertainties, in the model the bottom water carbon isotopes ($\delta^{13}C$ and $\Delta^{14}C$) response lags the sedimentary Pa/Th response by a few hundred years.

1 Introduction

Understanding rapid climate changes is key to understand the different natural modes of ocean circulation as they provide information about internal climate variability and climate sensitivity to perturbations. Indeed, during the last glacial, rapid and high-amplitude atmospheric temperature changes over Greenland of about 8 to 15°C in less than 300 years are associated with only small changes in radiative forcing (Kindler et al., 2014). Changes in the Atlantic Meridional Overturning Circulation (AMOC) strength are thought to be one of the main drivers of these abrupt climate events (see Lynch-Stieglitz, (2017) for a review), but the underlying mechanisms remain elusive. Available AMOC records based on observations only cover a few decades, thus identifying the processes controlling AMOC changes can only be achieved from the study of long-term variations (Smeed et al., 2014), which relies on the analysis of indirect evidence (paleoproxies).

To date, among the numerous tracers available (e.g. benthic $\delta^{18}O$, Nd isotopes, Cd/Ca or sortable silts), the sedimentary ($^{231}Pa_{xs,0}/^{230}Th_{xs,0}$) ratio (hereafter Pa/Th) and carbon isotopes ($\delta^{13}C$, $\Delta^{14}C$) are key tracers to reconstruct and quantify past circulation patterns and water mass flow rates.

The Pa/Th is the ratio of the ^{231}Pa and ^{230}Th activities (decays per time unit) at the deposition time that are derived from the water column scavenging. The Pa/Th ratio can be used as a kinematic circulation proxy (François, 2007; McManus et al., 2004). In short, ^{231}Pa and ^{230}Th are homogeneously produced in the water column at known rates with a known production ratio of 0.093 and are then transferred to the underlying sediments by particle scavenging (see (François, 2007) for a review). The two isotopes have different residence times in the water column (50-200 years for ^{231}Pa and 10-40 years for ^{230}Th (Henderson and Anderson, 2003)). Thus, while ^{230}Th is rapidly transferred to the sediment, ^{231}Pa can be partly transported by water mass advection along the large-scale ocean circulation. Consequently, the sedimentary Pa/Th activity ratio can be used as a proxy of water-mass advection rate. In the Atlantic, low sedimentary Pa/Th ratios (*e.g.* 0.04 for the modern North Atlantic (Yu et al., 1996)) are diagnostic of an active overturning, while Pa/Th ratios close or equal to the production ratio indicate a sluggish water mass or a marked overturning circulation slowdown (*e.g.* (Böhm et al., 2015; François, 2007; McManus et al., 2004; Waelbroeck et al., 2018)). Yet, Pa and Th scavenging to the sediment is sensitive to changes in vertical particle flux and composition; hence the sedimentary Pa/Th circulation signal could be partly biased by a particle-related signal (*e.g.* (Chase et al., 2002, 2003; Lippold et al., 2009)). In addition, sedimentary Pa/Th is derived from bulk sediment measurements and requires the estimation of the contributions of the detrital and authigenic fractions to the ^{231}Pa and ^{230}Th budgets. We have recently shown that this estimation can lead to significant uncertainties on the reconstructed patterns and amplitudes of the Pa/Th signal, especially in locations characterized by high terrigenous inputs (Missiaen et al., 2018). These potential caveats need to be tested and could complicate the evaluation of past circulation strength changes from Pa/Th measurements.

The carbon isotopes measured in foraminifer shells reflect the carbon isotopic content of the water mass in which they form and provide information about past water mass ventilation, in other words, the time elapsed since the tracked deep-water parcel has been isolated from the surface (*e.g.* (Lynch-Stieglitz et al., 2014; Skinner et al., 2014)).

More precisely, the water mass δ^{13}C signature depends on biological and physical processes. Carbon is exchanged between the surface waters and the atmosphere. In the surface waters, carbon is incorporated into the organic matter through biologic productivity. Both air-sea exchange and biological activity are responsible for isotopic fractionation between ^{12}C and ^{13}C (Siegenthaler and Münnich, 1981). Consequently, the surface water δ^{13}C signature varies with air-sea exchange efficiency and biological activity intensity. At depth, remineralization of organic matter releases ^{12}C to the water parcels, which are then mixed through large-scale ocean circulation. In the modern ocean, the global δ^{13}C distribution depicts a tight relation between the apparent oxygen utilization and the δ^{13}C signature of a given water mass (Eide et al., 2017). This observation lends support to the use of the δ^{13}C of benthic foraminifers as a proxy for ocean oxygen content and ventilation (Duplessy et al., 1988). However, benthic δ^{13}C does not solely record deep ventilation changes. As mentioned above, the δ^{13}C signature of a deep-water mass depends on several processes: its value before the water left the surface mixed layer, the intensity of the biological activity in the mixed layer, the remineralization intensity at depth and finally the circulation path and strength. Thus, benthic δ^{13}C records multiple processes, which complicates its interpretation in terms of past deep ocean ventilation and circulation changes.

Radiocarbon is produced in the upper atmosphere and enters into the ocean via air-sea exchange with surface waters. As soon as a water parcel is isolated from the surface, its ^{14}C content starts to decrease exponentially with time due to radioactive decay (half-life of ^{14}C = 5,730 ± 40 years (Godwin, 1962)). Thus, by determining the ^{14}C age of benthic foraminifer samples of independently known calendar age, one can reconstruct past ocean ventilation, (*e.g.* (Skinner and Shackleton, 2004; Thornalley et al., 2015)). However, the interpretation of a water mass radiocarbon age is complicated by temporal variations in ^{14}C production in the upper atmosphere and air-sea exchange efficiency. Indeed, since radiocarbon is only produced in the atmosphere and transferred to the ocean via air-sea exchange, the surface waters have an older radiocarbon age than the contemporaneous atmosphere. This radiocarbon age difference between the surface waters and the atmosphere (termed the surface reservoir age) can vary with space and time according to variations in air-sea exchanges efficiency, especially in the North Atlantic region (see (Bard et al., 1994; Bondevik et al., 2006; Thornalley et al., 2011; Waelbroeck et al., 2001)). Those

variations are still poorly constrained, and complicate the interpretation of deep water radiocarbon content (expressed as $\Delta^{14}C$ in ‰) in terms of past ocean ventilation and circulation changes (*e.g.* (Adkins and Boyle, 1997)).

Pa/Th, benthic $\delta^{13}C$ and $\Delta^{14}C$ can provide useful information about past ocean circulation flow rate, geometry and ventilation. Yet, as highlighted above, each proxy has its own caveats. To overcome the limitation of each proxy taken separately and gather more detailed information about past ocean circulation, paleoceanographers started to conduct multi-proxy studies, producing different proxy records on the same sedimentary archive. Moreover, this approach also enables one to investigate phase relationships between the different proxies (Burckel et al., 2015; Waelbroeck et al., 2018). Indeed, current dating uncertainties in marine cores are generally less than 150 y between 0 and 11 ky cal BP (ka), increasing to ~400 y between 11 and 30 ka and ranging from ~600 to 1100y between 30 and 40 ka (Waelbroeck et al, submitted). Such uncertainties usually prevent the inference of phase relationships between proxy records from different marine cores, hence limiting the benefit of the multi-proxy approach.

Different proxies can bring conflicting information about past ocean circulation and reconstructing basin-scale ocean water-mass reorganization requires to compile proxy records from different locations. Despite some recent paleoproxy compilation efforts (Lynch-Stieglitz et al., 2014; Ng et al., 2018; Zhao et al., 2018), the amount of data available remains too sparse to constrain the state and evolution of the ocean circulation in 3-D across abrupt climate events. One way to better understand existing paleo-records and overcome the scarcity of paleo-data is to use climate models able to simulate the evolution of different proxies in a consistent physical framework. Such work could help to explain why some events are not recorded or recorded differently at a given location. Climate models are also useful as they enable to analyze the spatial and temporal response of a proxy to changes of ocean circulation.

Because of its key role in the climate system, the carbon cycle has been modelled and heavily studied in the past decades (Friedlingstein et al., 2006; Orr et al., 2001). More recent studies simulate the evolution of carbon isotopes, and in particular ^{13}C and ^{14}C, under pre-industrial or glacial conditions (Bouttes et al., 2015; Brovkin et al., 2002; Menviel et al., 2017; Tschumi et al., 2011). The ^{231}Pa and ^{230}Th tracers have also been implemented in climate models. The simplest approaches used 2D models (Luo et al., 2010; Marchal et al., 2000) or 3D models but contained oversimplifications, notably in the particles representations (Siddall et al., 2005, 2007). Latest published developments focused on an improved representation of particle fluxes and scavenging scheme (Gu and Liu, 2017; van Hulten et al., 2018; Rempfer et al., 2017). However, these recent developments either suffer from the coarse resolution of the ocean model (Rempfer et al., 2017) which contains only 36 x 36 grid cells (latitude-longitude), or conversely cannot simulate 1,000 years in reasonable computation time (van Hulten et al., 2018). To our knowledge, there has not been any study so far that considered the geographical distribution and the temporal evolution of combined proxies such as Pa/Th, $\delta^{13}C$ and $\Delta^{14}C$.

We further investigate the spatial and temporal structure of multi-proxy response to an abrupt circulation change with a climate model. For that purpose, we have implemented the production and scavenging processes of ^{231}Pa and ^{230}Th in the climate model of intermediate complexity iLOVECLIM. To date, the model is able to simulate the evolution of three ocean circulation proxies: Pa/Th, $\delta^{13}C$ and $\Delta^{14}C$. We also developed an analysis method that gives information about the magnitude and timing of the proxy response in the Atlantic Ocean. In this study, we address the following questions. 1) What is the response of each proxy to an imposed circulation change? 2) What is the timing and sequence of the proxy responses? How do they vary with regions and water depth in the Atlantic Ocean? 3) How can the modelled multi-proxy response help to interpret the paleoproxy records?

2 Material and methods

2.1 Model description and developments

We use the Earth system model of intermediate complexity iLOVECLIM, which is a code fork of the LOVECLIM model (Goosse et al., 2010). It includes a representation of the atmosphere, ocean, sea ice, terrestrial biosphere vegetation, as well as

the carbon cycle. The ocean component (CLIO) consists of a free-surface primitive equation ocean model (3° x 3° horizontal grid, 20 depths layers) coupled to a dynamic-thermodynamic sea-ice model. iLOVECLIM includes a land vegetation module (VECODE) (Brovkin et al., 1997) and a marine carbon cycle model (Bouttes et al., 2015) both computing the evolution of ^{13}C and ^{14}C. Previous work has shown that the simulated oceanic $\delta^{13}C$ and $\Delta^{14}C$ distribution is in reasonable agreement with observations and with available GCM simulations (Bouttes et al., 2015). We have implemented ^{231}Pa and ^{230}Th in the iLOVECLIM model following the approach of (Rempfer et al., 2017) albeit without including an explicit parametrization of boundary and bottom scavenging as detailed in the following. In the model, ^{231}Pa and ^{230}Th are homogeneously produced in the ocean by radioactive decay of their respective uranium parents. They are removed from the water column by adsorption on settling particles (reversible scavenging). Their radioactive decay is also taken into account. In its current version, iLOVECLIM does not explicitly simulate the biogeochemical cycle of biogenic silica (opal), which is thought to be an important scavenger for ^{231}Pa (*e.g.* (Chase et al., 2002; Kretschmer et al., 2010)). Therefore, we used prescribed and constant particles concentration fields obtained running the PISCES biogeochemical model coupled to NEMO ocean model (van Hulten et al., 2018). Previous work has shown that these particle fields are reasonably consistent with present day observations (van Hulten et al., 2018) and that a set-up with fixed particles is able to capture the major features (Gu and Liu, 2017). Like in Bern 3D (Rempfer et al., 2017; Siddall et al., 2005, 2007) and CESM (Gu and Liu, 2017), we considered one particle size with a unique sedimentation speed of 1000 m/y. We consider that Pa and Th interact with three particles types: $CaCO_3$, POC and biogenic silica, the role of lithogenic particles in Pa and Th scavenging having been questioned (van Hulten et al., 2018; Siddall et al., 2005). The conservation equations for dissolved and particulate ^{231}Pa and ^{230}Th activities are the following (Rempfer et al., 2017):

$$\frac{\partial A_d^j}{\partial t} = T(A_d^j) + \beta^j + K_{desorp}^j.A_p^j - (K_{adsorp}^j + \lambda_j).A_d^j \,, \quad (1)$$

$$\frac{\partial A_p^j}{\partial t} = T(A_p^j) - \frac{\partial (w_s.A_p^j)}{\partial z} - (K_{desorp}^j + \lambda_j).Ap^j + K_{adsorp}^j.A_d^j \,, \quad (2)$$

Where A_d^j and A_p^j are respectively the dissolved and particle-bound activities ($dmp.m^{-3}.y^{-1}$) of isotope j (^{231}Pa or ^{230}Th), β^j ($dpm.m^{-3}.y^{-1}$) is the water column production of isotope j by radioactive decay of its uranium parent, λ_j (y^{-1}) is the decay constant of isotope j, w_s ($m.y^{-1}$) is the particle settling speed, K_{adsorp}^j and k_{desorp}^j (y^{-1}) are the adsorption and desorption coefficient of isotope j onto particles, respectively, T is the tracer balance evolution term ($dpm.m^{-3}.y^{-1}$) resulting from the water mass advection and diffusion terms computed by the CLIO ocean model. The values used in this study for each of the above-cited parameters are compiled in Table 1.

As in Bern 3D (Rempfer et al., 2017), we chose to apply a uniform desorption coefficient denoted K_{desorp} hereafter. However, the adsorption coefficient depends in our model on the particle concentration and composition of each location and is calculated with the following equation (Rempfer et al., 2017):

$$K_{adsorp}^j(\theta,\Phi,z) = \sum_i \sigma_{i,j}.F_i(\theta,\Phi,z) \,, \quad (3)$$

where θ is the latitude, Φ the longitude, z the water depth, $\sigma_{i,j}$ the scavenging efficiency for isotope j on particle type i ($m^2.mol^{-1}$), and F_i is the particle flux ($mol.m^{-2}.y^{-1}$).

2.2 Model tuning and validation

The scavenging efficiency $\sigma_{i,j}$ is related to the partition coefficient K_d, which defines the proportion of each isotope (^{231}Pa or ^{230}Th) lodged in the dissolved phase or bound to particles. Therefore one K_d can be defined for each isotope and each particle type considered in the model ($K_{d(i,j)}$, j representing the isotope Pa or Th and i the particle type).

$$Kd_{(i,j)} = \frac{\sigma_{i,j} \times w_s \times \rho_{sw}}{M_{(i)} \times k_{desorp}} \,, \quad (4)$$

where $K_{d(i,j)}$ is the partition coefficient for isotope i for particle type j, $\sigma_{i,j}$ is the corresponding scavenging efficiency, w_s is the settling speed, K_{desorp} is the desorption coefficient, $M_{(i)}$ is the molar mass of particle type i (i.e. 12 $g.mol^{-1}$ for POC, 100.08

g.mol^{-1} for $CaCO_3$ and 67.3 g.mol^{-1} for opal) and ρ_{sw} is the mean density of sea water (constant fixed to 1.03 10^6 g.m^{-3}). Additionally the way each particle type fractionates the Pa and the Th is defined by the fractionation factor $F(Th/Pa)_j$.

$$F(Th/Pa)_i = \frac{Kd_{(Th,i)}}{Kd_{(Pa,i)}} = \frac{\sigma_{(Th,i)}}{\sigma_{(Pa,i)}}, \quad (5)$$

K_d and fractionation factors (F(Th/Pa)) have been measured for both radionuclides in various areas of the modern ocean and they show a rather large distribution (see Table S1) (Chase et al., 2002; Hayes et al., 2015). Consequently, these values are currently considered as tunable parameters in modelling studies (Dutay et al., 2009; Gu and Liu, 2017; van Hulten et al., 2018; Marchal et al., 2000; Rempfer et al., 2017; Siddall et al., 2005). Considering three particle types for both radionuclides, there are thus six tunable $\sigma_{i,j}$ parameters in our model.

To efficiently sample our parameter space, we used a Latin Hypercube Sampling (LHS) methodology (https://CRAN.R-project.org/package=lhs). In order to only select parameters values consistent with observed F(Th/Pa), we chose to use the couples $\{\sigma_{(Th,j)}, F(Th/Pa)_i\}$ as input parameters for the LHS. The value of $\sigma_{Pa,i}$ is then deduced from those two following equation (Eq. 5). The parameter ranges used in the LHS are given in Table S2. The LHS allowed a relatively good exploration of the parameter space with a relatively small number of model evaluations. We performed 60 tuning simulations of 1,000 years each under pre-industrial boundary conditions (i.e. orbital parameters, ice-sheets configuration and atmospheric gas concentrations), as described in (Goosse et al., 2010).

Consistently with previous modelling studies (van Hulten et al., 2018), this simulation length was sufficient for Pa and Th to reach an approximate steady state at the surface and in the deeper ocean. The model performance was evaluated by comparing outputs with present day particulate and dissolved water column Pa and Th measurements compiled in the GEOTRACES intermediate data product 2017 (Schlitzer et al., 2018) as well as sedimentary Pa/Th core tops data as compiled in (van Hulten et al., 2018) and references therein. We selected the ensemble member that best fits the observational constraints using 5 metrics corresponding to the Root Mean Square Error (RMSE) between observation data and the closest model grid cell average for particulate and dissolved Pa and Th as well as sedimentary Pa/Th (see text S1 for additional information). Table 2 presents the best-fit σ_{ij} values. The best fit simulation is then used to investigate the multi-proxy response to abrupt circulation changes.

2.3 Experimental design

With the best fit σ_{ij} values (see Table 2), we ran our model for 5,000 years under Pre Industrial (PI) conditions (as described in (Goosse et al., 2010)) from a simulation with an equilibrated carbon cycle (Bouttes et al., 2015). The result of this equilibrium simulation is used as a starting point to perform hosing experiments of 1,200 years duration. The freshwater was added in the Nordic Seas following the approach described in (Roche et al., 2010). Each simulation contains three phases: a control phase (300 years), a hosing phase (300 years) and a recovery phase (600 years). The control phase is used to assess the natural variability of the circulation and associated proxies under the PI climate state.

3 Results

3.1. Model-data comparison under pre-industrial conditions

The main goal of our study is to assess the response of two carbon-based proxies ($\delta^{13}C$, $\Delta^{14}C$) and of the Pa/Th to an abrupt circulation change in a physically consistent framework. This work represents a first step toward a better understanding of marine multi-proxy records across the last glacial abrupt events. Therefore, our model-data comparison focuses on the Atlantic ocean, where the Pa/Th can be used as a kinematic circulation proxy (*e.g.* (François, 2007; McManus et al., 2004)). and on the simulated bottom particulate Pa and Th activities which can be directly compared to the Pa/Th ratio recorded in marine sediments. The water column concentration results are presented in the supplementary text S2 and Figures S1 to S3.

The particle-bound Pa/Th of the deepest oceanic model grid cells is shown in Figure 1. The observations from core-top data are superimposed as circles. Even if the observational dataset is somewhat patchy, it generally shows lower sedimentary Pa/Th ratios (0.04 or lower) in the basin interiors compared to the coastal areas. Another interesting feature is the high sedimentary Pa/Th values in the Southern Ocean between 50 and 75°S (opal belt), where Pa is heavily scavenged to the sediments by opal. Our model generates higher sedimentary Pa/Th in this region compared to the deep basin interior but our modelled opal belt stands slightly northward compared to the observations (Figure 1). In our best fit simulation, the adsorption/desorption coefficients fall in the upper range of observations (see Table 2, Table S1), therefore, Pa and Th are very effectively scavenged to the sediments. Besides, while Pa is mostly scavenged by the opal particles, Th mainly reaches the sediments with $CaCO_3$ particles (see SOM for detailed information). Overall, these results are comparable with GCM outputs (van Hulten et al., 2018). The modelled values display the first order characteristics observed in the modern ocean and the sediment core tops. In the following section, we test the sensitivity of the simulated sedimentary Pa/Th to abrupt circulation slowdown (hosing experiments).

3.2 Multi proxy response to an abrupt circulation slowdown

We added a freshwater flux of 0.3 Sv in the Nordic Seas during 300 years, which was sufficient to cause a drastic circulation reduction (Roche et al., 2010). Under PI conditions, the maximum of the AMOC stream function is about 15 Sv in our model. During the hosing, North Atlantic water formation drops to nearly 0 Sv and the upper overturning cell completely vanishes (see Figure S4). The AMOC recovers ~200 y after the end of the water hosing and displays a small overshoot with the maximum Atlantic meridional stream function exceeding 20 Sv around 900 years (Figure 5).

We evaluate the response of Pa/Th, $\delta^{13}C$ and $\Delta^{14}C$ to the hosing in the Nordic Seas as follows. We identify, for each model grid cell and each proxy, the simulation periods exceeding 80 years during which the proxy values are outside of their natural variability range. The latter is defined as the proxy variance (2σ) under PI conditions over the first 300 years of the simulation (control phase-see Figure 2). In most cases, 0, 1 or 2 periods of significant response are detected. In some grid cells with high proxy variability, we detect up to 4 periods of significant proxy response, which are difficult to relate either with the hosing or overshoot timing of our simulation. Consequently, we excluded the grid cells depicting more than two periods of significant response from the subsequent analysis. For the time series containing two or less periods of interest, we call "time of maximum response", the simulation year for which the absolute difference between the proxy value and mean proxy value during the control phase of the simulation is maximal. The proxy value at the time of maximum response is denoted "proxy response" in the following (Figure 2). The single or dual proxy response is compared to the control proxy value (*i.e.* the mean proxy value over the 300 first years of the simulation). Figure 3 represents the zonal mean proxy response in the western Atlantic basin, the delimitation between the two basins being defined by the position of the mid-Atlantic Ridge (see Figure S5 and S6 for Eastern basin).

The $\delta^{13}C$ and $\Delta^{14}C$ only display one single response in the deep western Atlantic whereas the Pa/Th generally displays one or two responses in this part of the basin. Generally, the single or the first response of each proxy has the same geographical pattern (Figure 3A. and B. early response) while in the case of two distinct responses, the late response has a radically different pattern (Figure 3 B. late response). For $\delta^{13}C$ and $\Delta^{14}C$, the late response corresponds to a general increase in the western Atlantic basin. For Pa/Th, the late response pattern consists in increased values in the southern Atlantic and decreased values in the North-Atlantic and is the opposite of the early response pattern. For the three proxies, the late response pattern is generally consistent with the circulation overshoot observed around 900 simulated years.

Considering that the single and the first responses mostly represent the proxy response to the hosing, a consistent proxy response is observed in the following three zones of the western Atlantic basin: the surface and intermediate waters (0-1,500 m), the deep North-Atlantic waters (> 2,000 m), and the Southern Ocean (south of 30°S). In the surface waters and intermediate waters the proxy response pattern is as follows. The $\delta^{13}C$ decreases in the first 500 m and then increases around 1,000 m. The $\Delta^{14}C$ increases

from the surface to 1,500 m and Pa/Th displays no clear trend. In the deep North-Atlantic waters, the $\delta^{13}C$ and $\Delta^{14}C$ decrease while the Pa/Th generally increases, the three proxies reflecting a reduction of the North Atlantic Deep Water (NADW) flow rate. In terms of magnitude, we observe the strongest proxy response between 60°N and 40°N and between 1,500 and 3,000 m for the three proxies. In the Southern Ocean, the Pa/Th generally decreases, except in the deep southern basin (between 40 and 60°S below 3,000 m). The $\delta^{13}C$ and $\Delta^{14}C$ display a dipole pattern increasing at the surface and decreasing at depth. For $\delta^{13}C$, the depth boundary is around 1,500 m while for $\Delta^{14}C$ the depth boundary is ~1,500 m north of 50°S and reaches 3,000 m south of 40°S.

Looking at the proxy time of response (Figure 4), we observe significantly different patterns for Pa/Th and the carbon isotopes. The $\delta^{13}C$ and $\Delta^{14}C$ time of response increases with depth: in the surface and intermediate waters the response occurs roughly 300 years after the beginning of the fresh water addition, around 3,000 m the response is delayed by 150 years and towards the ocean bottom the delay increases up to 600 years. On the contrary, the Pa/Th displays much smaller time of response, the timing of the Pa/Th response being generally synchronous with the minimum of the stream function 300 years after the beginning of the freshwater addition. Consequently, in most of the western Atlantic basin, the response of the carbon isotopes lags the Pa/Th response by a few hundred years, especially in the deeper waters.

In the eastern Atlantic basin the general pattern of the proxy response is similar to that of the western basin (Figure S4 - Figure S5). However, we note that the $\delta^{13}C$ has frequently more than a single response, especially at depths > 2,000m. The $\delta^{13}C$ displays overall the same pattern as in the western basin except in the south deep basin (between ~20 and 30 °S – below 2,500 m) in the case of a dual response. The $\Delta^{14}C$ shows the same pattern as in the western basin, with increased values during the hosing in surface and intermediate waters and lower values at depth. Besides, the Pa/Th has a more complex pattern with a large increase in the arctic basin, a moderate increase in the tropical basin and a decrease in the northern and southern basins through the entire water column. Concerning the times of response, the same pattern as in the western ocean is observed. Interestingly, we note that the $\Delta^{14}C$ has longer times of response in the eastern basin compared to the western basin in the case of one single response (Figure S5). This is consistent with a lower ventilation of the eastern basin associated with a lower penetration of the NADW relative to the situation in the western boundary current.

Overall, the objective analysis of the multi-proxy response allows the identification of 3 regions with different reaction patterns:
i) The clearest proxy response happens in the North western Atlantic between 40°N and 60°N, 1,000 and 5,000 m. In this area, the $\delta^{13}C$ and $\Delta^{14}C$ display marked decreases during the hosing while the Pa/Th significantly increases. Another interesting feature is that the $\delta^{13}C$ and $\Delta^{14}C$ lag the Pa/Th by about 200 y (Figure 5-A). In our model, this zone corresponds to the region of NADW formation and first portion of southward flow at depth.
ii) In the tropical intermediate and surface waters, $\delta^{13}C$ and $\Delta^{14}C$ increase during the hosing compared to the reference value while Pa/Th generally displays no clear reaction or very low amplitude increase (Figure 5-B).
iii) In the Southern Ocean (south of ~30°S), below 3,000 m, $\delta^{13}C$ and $\Delta^{14}C$ display a progressive decrease, while Pa/Th slightly increases during the hosing. No lag between the Pa/Th and the carbon isotopes response is observed (Figure 5-C). In our model, this zone corresponds to the Antarctic Bottom Water (AABW).

4 Discussion

The need for a more direct and efficient comparison between modelled proxies, easily related to modelled physical variables (e.g. stream function and currents) and observed paleoproxy data motivated the implementation of several tracers in climate models. In this study we have fingerprinted the response of carbon isotopes ($\delta^{13}C$ and $\Delta^{14}C$) and Pa/Th to an abrupt circulation slowdown subsequent to freshwater addition in the Nordic Seas. In short, our simulations show that the three proxies considered do not systematically respond simultaneously and in a simple manner to a given oceanic circulation change. Instead, the proxy

responses show a strong spatial variability in the Atlantic basin tightly related to the water mass mostly bathing the considered location. Besides, in a large part of the western Atlantic, the carbon isotopes response lags the Pa/Th response by about 200 years, the actual time lag displaying marked spatial variability (Figure 4 and 5). Our simulations thus indicate that a given circulation change event is not likely to produce a synchronous response, either for a given proxy in different regions of the Atlantic basin, or for different proxies taken at the same location (i.e. sediment core), potentially complicating proxy data interpretation. In this section, we discuss the potential underlying physical mechanisms and compare our results with available model results and proxy data.

4.1 The lag of carbon isotopes, underlying physical mechanisms

One of the most interesting features of our simulations is that the $\delta^{13}C$ and $\Delta^{14}C$ response lags the Pa/Th response by a few hundred years, in particular in the Northwest Atlantic, bathed by the NADW, suggesting a shorter time of response for the Pa/Th compared to carbon isotopes.

First, let us point out that the physical mechanisms leading to the $\delta^{13}C$, $\Delta^{14}C$ and Pa/Th signals are fundamentally different. On the one hand, Pa and Th have very short residence times in the water column. In our simulations, the particles fluxes remain prescribed and constant. Therefore, any change of the particle production due to the freshwater forcing is not accounted for and does not impact the sedimentary Pa/Th in our simulations. Instead, the sedimentary Pa/Th in the North-Atlantic purely reflects the capacity of the NADW to transport Pa further south. Thus, the NADW cessation rapidly translates in a sedimentary Pa/Th increase, which is resorbed as soon as the NADW resumes and is able to transport Pa again, at the end of the hosing period (i.e. after year 600). On the other hand, the oceanic carbon isotopes depend not only on circulation changes, but also on the biological activity and air-sea exchanges. Carbon is further actively partitioned between different reservoirs (terrestrial biosphere, ocean and atmosphere), hence the longer time needed by carbon isotopes to adjust to any change.

In our simulations, the freshwater perturbation lasts 300 years and the NADW formation is stopped for about 100 years (Figure 5), which is likely too short for the isotopic systems to fully adjust to the change. However, our experimental set-up is relevant to the study of centennial to millennial scale events (DO or Heinrich events) across which the climate and isotopic systems likely did not have the time to fully adjust either. In line with previous hosing experiments (e.g. (Kageyama et al., 2013; Mariotti et al., 2012; Menviel et al., 2008, 2015), the freshwater addition in the Nordic Seas produces a surface cooling of about 1°C associated with an increase of the CO_2 solubility in surface waters and a general marine productivity decrease in the North Atlantic. Subsequent to the NADW cessation, the nutrients accumulate in the Atlantic intermediate waters, shaping a negative $\delta^{13}C$ anomaly and its counterpart positive phosphate anomaly in the North Atlantic around 50°N (Menviel et al., 2015). In our simulations, the biological productivity or air-sea exchanges response peak around year 600, when the AMOC is the weakest (Figure S7). Therefore, the lag between the Pa/Th and carbon isotopes responses is not related to late biological or air-sea exchange responses themselves but rather to the time needed to transport the anomaly to the deep ocean. Indeed, in our simulations, the northern sourced $\delta^{13}C$ anomaly progressively spreads to the deep Atlantic basin and finally reaches the bottom ocean (> 4000 m) around year 800, about 200 years after the AMOC has reached its lower value (Figure S8).

4.2 Comparison to proxy data and previous modelling efforts

4.2.1 Context overview

From the modelling side, the response of carbon isotopes and Pa/Th to AMOC slowdown has so far been investigated in separate climate models. Unfortunately, experimental setups for the hosing strongly vary in terms of freshwater flux, duration and location from one publication to another, complicating quantitative comparison. Nevertheless, consistently with what is described in iLOVECLIM, the models generally simulate a marked Pa/Th increase in the Northwest Atlantic (Gu and Liu, 2017;

Rempfer et al., 2017; Siddall et al., 2007) and a decrease of $\delta^{13}C$ in response to the AMOC slowdown (e.g. (Menviel et al., 2015; Schmittner and Lund, 2015)).

From the data side, the best analog for our hosing experiments applied to a PI state would be the 8.2 ky cal BP event (Alley et al., 1997), attributed to the drainage of the glacial Lake Agassiz (Hoffman et al., 2012; Wiersma and Renssen, 2006). However, this event is of short duration (~300 years) and if some benthic $\delta^{13}C$ data are available (*e.g.* (Kleiven et al., 2008)), to date there is no sufficiently well-resolved $\Delta^{14}C$ and Pa/Th records covering this event.

The Heinrich events and DO-cycles are good candidates to compare with our hosing experiments because they are strongly related to freshwater fluxes in the North Atlantic (*e.g.* (Broecker et al., 1990; Hemming, 2004)) and associated with circulation changes that have been documented in $\delta^{13}C$, $\Delta^{14}C$ and Pa/Th records (Böhm et al., 2015; Henry et al., 2016; Lynch-Stieglitz, 2017; Waelbroeck et al., 2018). However, the available paleoproxy data is relatively sparse and the extensive time series are rare. In addition, to date there is no published combined Pa/Th, benthic $\delta^{13}C$ and $\Delta^{14}C$ record available for the same sediment core. Nevertheless, remarkably comprehensive multiproxy records are available for the Iberian margin (Gherardi et al., 2005; Skinner and Shackleton, 2004), the Brazilian margin (Burckel et al., 2015, 2016; Mulitza et al., 2017; Waelbroeck et al., 2018) and the Bermuda Rise (Böhm et al., 2015; Henry et al., 2016; Lippold et al., 2009; McManus et al., 2004). A common working hypothesis is to assume that these records represent the proxy evolution of the surrounding basin. Besides, some recent compilations (*e.g.* (Lynch-Stieglitz et al., 2014; Ng et al., 2018; Zhao et al., 2018)) bring some insight about the evolution of Pa/Th, benthic $\delta^{13}C$ and $\Delta^{14}C$ across the last 40 ky in the Atlantic Ocean.

However, our hosing experiments are not direct analogues of the millennial scale climate changes of the last glacial cycle because i) glacial millennial events occurred under glacial conditions whereas our simulations were run under PI conditions, ii) the Heinrich and DO events have distinct proxy patterns and cannot be entirely explained by a simple fresh water addition in the North Atlantic and iii) the freshwater inputs might have occurred in different locations across distinct millennial scale events (e.g. originating from the Laurentide or Scandinavian ice sheet) while in our experiment, the freshwater was only added in the Nordic seas. Furthermore, the sequence of mechanisms involved in Heinrich stadials is still under debate (Barker et al., 2015; Broecker, 1994) and these periods were likely subdivided in several distinct phases (Ng et al., 2018; Stanford et al., 2011).

Besides, the model set-up used in this study is rather crude. It uses fixed modelled particle fields and does not explicitly represent boundary or bottom scavenging by nepheloid layers. However, because the particle fields used show higher concentrations at the continental margins, a greater Pa and Th scavenging is achieved in the areas of observed boundary scavenging. Therefore, an additional parametrization for boundary scavenging might not be necessary. However, the absence of representation of preferential Pa scavenging by resuspended particles at the bottom in nepheloid layers (*e.g.* (Anderson et al., 1983; Gardner et al., 2018; Thomas et al., 2006)) has not been parametrized in our model and could explain the relatively high sedimentary Pa/Th values in the Northwest Atlantic offshore Newfoundland and Florida. Given the reasons above, we will only discuss the common/divergent trends rather than precise values between the paleodata and our model output.

4.2.2 General Atlantic features

The available paleodata display a consistent proxy evolution in the western Atlantic and in particular in the western boundary current. Deep Northwest Atlantic cores present the same Pa/Th pattern over the last 25 ky with a significant Pa/Th increase during HS1 (Ng et al., 2018). A ~0.4 ‰ benthic $\delta^{13}C$ decrease is observed for some Heinrich events in deep and intermediate Atlantic waters (Lynch-Stieglitz et al., 2014). Finally, several coral and foraminifers ^{14}C records also depict a decreased ^{14}C (decreased $\Delta^{14}C$) content of deep waters and increased deep ventilation ages during HS1 (Chen et al., 2015; Skinner et al., 2014). While no major East-West difference has been highlighted concerning the carbon isotopes, Pa/Th response seems less clear in the eastern Atlantic basin compared to the western boundary current. While some East Atlantic cores located close to

the Mid-Atlantic ridge and the Iberian margin reproduce the amplitude of Pa/Th variations observed in the western basin, two other eastern records display no millennial scale variability (Ng et al., 2018).

In line with the paleoproxy data, our model results show a coherent and significant $\delta^{13}C$ and $\Delta^{14}C$ decrease in the deep western Atlantic. Overall the same response pattern is obtained in our model in the eastern Atlantic basin with the exception of the deep South East Atlantic (between ~20 and 30 °S – below 2500 m). In this region, we observe a slight increase of the $\delta^{13}C$ during the early response in the case of a dual response while the $\Delta^{14}C$ decreases during the single or early response. We note that the amplitude of this early $\delta^{13}C$ increase is rather small compared to the late $\delta^{13}C$ decrease. Moreover, in this region, the time of response is rather short (~100 – 150 y). We argue here that in this particular region the $\delta^{13}C$ displays a two-phase response, the actual long-term response corresponding to the late response.

In the surface and intermediate waters, the modelled $\delta^{13}C$ decreases above 500 m and then increases around 1,000 m while $\Delta^{14}C$ generally increases from the surface to 1,500 m (Figure 3). This $\delta^{13}C$ pattern is consistent with changes in productivity reported in previous hosing experiments. Indeed, due to changes in winds and upwelling intensity and subsequent changes in nutrient availability, the productivity generally decreases in the North and equatorial Atlantic (Menviel et al., 2008). Therefore, the $\delta^{13}C$ of the photic zone decreases and the $\delta^{13}C$ of the remineralization zone (~1,000 m) increases as the export from ^{13}C depleted carbon is reduced during the hosing compared to the PI equilibrium state. As reported in other model studies, the increased $\Delta^{14}C$ in the upper ocean reflects the accumulation of radiocarbon in the atmosphere and the upper ocean in the absence of carbon entrainment to deep water through North Atlantic deep-water formation (Butzin et al., 2005). The generally good ventilation state of the upper ocean indicated by both $\delta^{13}C$ and $\Delta^{14}C$ may also be related to an increase of the of vertical mixing (and ventilation) in the intermediate waters in the absence of North Atlantic deep convection cell (Schmittner, 2007). The pattern we obtain in the intermediate waters (Figure 3 and 5 B) is consistent with a $\delta^{13}C$ dataset on the Brazilian margin (Lund et al., 2015; Tessin and Lund, 2013) showing increasing $\delta^{13}C$ between 1,000 and 1,300 m and decreasing between 1,600 and 2,100 m water depth. These results are also fairly consistent with the modelled $\delta^{13}C$ described in (Schmittner and Lund, 2015), though our hosing experiments are fairly shorter (300 years vs 2,000 y).

In agreement with the Pa/Th data, the model simulates a clear Pa/Th increase in the NADW in the western basin while the results are more ambiguous in the eastern basin. Indeed, in the eastern basin, except at high northern latitudes, very small amplitude Pa/Th variations are observed, with increasing values in the equatorial zone and decreasing values elsewhere. Thus, our modelled Pa/Th response at the Iberian margin is very different from the Iberian margin record. The low amplitude of our Pa/Th response may arise from the absence of strong Pa advection towards the Southern Atlantic in relation with the East Equatorial Atlantic upwellings variations across the hosing experiment (Menviel et al., 2008). Alternatively, the absence of Pa/Th signal in the eastern basin could be due to an overestimation of the water fluxes that cross Gibraltar in the model. Indeed, the model resolution is rather coarse and the Gibraltar Straight is represented by a full ocean grid cell of 3 x 3 degrees, unrealistically impacting the simulated eastern Atlantic circulation. Additionally, the modelled Pa/Th displays interesting features in the Southern Atlantic and in the surface and intermediate waters (between 40°S and 40°N). In both cases, no reliable Pa/Th record is available because particles fluxes from the opal belt (southern Atlantic) and coastal areas (surface waters) overprint the Pa/Th circulation signal. In our model, we observe that the single and the early responses do not match, and that the response of the Pa/Th is rather fast (~100 -150 y) in the case of a dual response. This suggests that in this area, the Pa/Th displays a two-phase response to the freshwater addition and AMOC perturbation.

Further investigations about this two-phase response for Pa/Th and $\delta^{13}C$, in particular in the Southern Ocean, would require 1) monitoring of the detailed 3-D circulation pathway and carbon exchanges between the different reservoirs and 2) running experiments with increased hosing duration in order to better assess the proxy response to a sustained (~1,500 y) AMOC shutdown.

4.3.2. Bermuda Rise and Brazilian margin multi-proxy records

The Brazilian margin and the Bermuda Rise are located in the western boundary current and display similar proxy patterns. The Pa/Th increases from ~0.06 to the production ratio (0.093) or even above while the $\delta^{13}C$ decreases by ~0.5 ‰ across the Heinrich events. Similar Pa/Th and benthic $\delta^{13}C$ changes, but of smaller/reduced amplitude, are also observed for the DO stadials.

Below, we examine our modelled time series in the Bermuda Rise basin (~34°N-58°W, >4,300m) (Figure 6). The presented time series correspond to the average of 9 model grid cells and are representative of the time series of the deep western basin (see Figure 5 and Figure 6). The simulated Pa/Th significantly increases between year 350 and year 850 of the simulation, consistently with the decrease of the maximum Atlantic stream function (Figure 6). The simulated Pa/Th approaches the production ratio of 0.093 at year 600, and the maximum stream function is close to zero from y 400 to 600, which is consistent with a sedimentary Pa/Th reaching the production ratio in the case of an AMOC shutdown. The simulated Pa/Th change has a moderate amplitude of 0.015 Pa/Th units (from ~0.075 to 0.090) but is significant with respect to the natural variability recorded during the 300 first years of the simulation under PI conditions. Our simulated $\delta^{13}C$ decreases from ~0.62 ‰ to ~0.5 ‰, reaching the minimum around year 900, i.e. 600 years after the beginning of the hosing. The simulated $\delta^{13}C$ decrease has a moderate amplitude of ~0.12 ‰ but is significant with respect to the natural variability recorded in the control first 300 years of the simulation. Although the trend of the simulated and observed proxy response is the same, their absolute values differ. In our simulated record, the Pa/Th value associated with the modern circulation scheme is around 0.075, which is significantly higher than the value actually measured at the Bermuda Rise or Brazilian margin sites: ~0.06. For both proxies, the simulated amplitude of change is much smaller than the amplitude recorded in the paleodata across the Heinrich events: the modelled $\delta^{13}C$ decrease is around 0.12 ‰ while it is 0.5 ‰ in the paleodata; the modelled Pa/Th change is ~0.015 while it is ~0.03 in the paleodata. This might be a consequence of the short duration of the fresh water forcing and induced reduction in AMOC (for carbon isotopes) and to poor particle representation along the Northeast American coast (for Pa/Th).

The lead/lag relationship between Pa/Th and benthic $\delta^{13}C$ was previously examined on data both at the Brazilian margin and the Bermuda Rise with opposite conclusions: at the Brazilian margin the Pa/Th was found to lead $\delta^{13}C$ by about 200 years (Waelbroeck et al., 2018), while at the Bermuda Rise, the Pa/Th was found to lag $\delta^{13}C$ by about 200 years (Henry et al., 2016). However, the latter result must be interpreted with caution since the cross-correlation method used to evaluate the lead or lag relationships in (Henry et al., 2016) has been designed for signals that are stationary in time and is thus is not suitable to analyze non-stationary climatic signals (Waelbroeck et al., 2018). Therefore, the paleodata seem to suggest a lead of the Pa/Th response with respect to the carbon isotopes response in the western boundary current. However, this observation may simply reflect the impact of bioturbation on sediment archives. Indeed, even if the two proxies are recorded in a single sediment core, it is important to note that both proxies are not hosted by the same sediment fraction: the Pa and Th being preferentially adsorbed on the fine grain particles (<100 μm, (Chase et al., 2002; Kretschmer et al., 2010; Thomson et al., 1993)) while $\delta^{13}C$ and $\Delta^{14}C$ are measured on foraminifer shells that correspond on larger particle sizes (> 150 μm). It has been shown that bioturbation could affect different particle sizes differently (*e.g.* (Wheatcroft, 1992)). Therefore Pa/Th and carbon isotopes could be affected by bioturbation in a different way, and the 200 years Pa/Th response lead on carbon isotopes observed in Brazilian margin sediments could then solely be explained by sediment bioturbation, as suggested in (Waelbroeck et al., 2018). In contrast, in our model we observe a systematic lead of the Pa/Th response with respect to the carbon isotopes in the NADW. Therefore, our model suggests that this Pa/Th lead may be a feature of the proxy response to millennial scale variability and is not necessarily an artefact due to the marine core bioturbation.

Conclusions and perspectives

We have implemented the ^{231}Pa and ^{230}Th tracers in the climate model of intermediate complexity iLOVECLIM. The new Pa/Th module simulates dissolved and particulate ^{231}Pa and ^{230}Th concentrations with a quality comparable to GCMs under PI equilibrium.

To date, the model is able to simulate the evolution of $\delta^{13}C$, $\Delta^{14}C$ and Pa/Th over thousands of years in a consistent physical framework and in a reasonable computation time (~800 years per 24h). We tested and fingerprinted the response of these three proxies to an imposed and abrupt circulation change by adding freshwater in the Nordic seas. The proxy response displays high spatial and temporal variability but three patterns of proxy response, tightly related to the main Atlantic water masses, can be identified. In intermediate waters, the Pa/Th and $\Delta^{14}C$ show a slight increase while the $\delta^{13}C$ significantly increases. In AABW, the three proxies display consistent and synchronous responses: the Pa/Th increases while the $\delta^{13}C$ and $\Delta^{14}C$ decrease, corresponding to a reduced circulation and ventilation of the water mass. Finally, in NADW, the Pa/Th increases while the $\delta^{13}C$ and $\Delta^{14}C$ decrease, with a lag of about 200 years between the Pa/Th and carbon isotopes responses. Our simulations show that this lag is induced by the different mechanisms producing the proxy records. Indeed, since our model set-up uses prescribed particles fields, the sedimentary Pa/Th in the North Atlantic basin is purely driven by the capacity of the ocean circulation to transport Pa further south. On the contrary, the carbon isotopes- are impacted by multiple processes, such as biological productivity, remineralization and air-sea exchanges, and the anomaly formed in the intermediate North-Atlantic takes time to be exported toward the deep basin.

Despite the crudeness of the model set-up and incomplete representation of the processes governing Pa and Th scavenging in the water column, the main features of our modelled Pa/Th and carbon isotopes responses are consistent with the available paleo proxy record. We observe i) coherent proxy response along the Atlantic western boundary current for the three proxies consisting in a significant Pa/Th increase and $\delta^{13}C$ and $\Delta^{14}C$ decrease, ii) distinct proxy responses for intermediate and deep waters for $\delta^{13}C$ and $\Delta^{14}C$, and iii) a constitutive lag between the Pa/Th and carbon isotopes, consistent with a multi-proxy record from the Brazilian margin. Our study therefore suggests that a given circulation change event does not likely produce a synchronous response, either for a given proxy in different regions of the Atlantic basin, or for different proxies taken at the same location (i.e. sediment core), potentially complicating proxy data interpretation. Future work is required to evaluate the multi-proxy response in more realistic numerical experiments, using glacial boundary conditions and coupled/interactive particle fields. In addition, a more complete dataset containing multi-proxy records is needed to achieve a more complete model-data comparison.

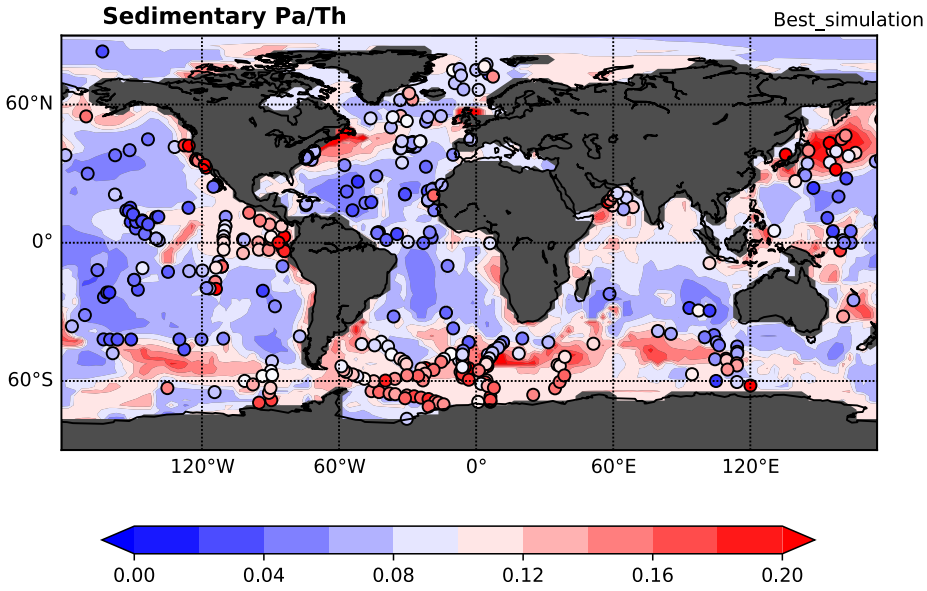

Figure 1: Map showing the particulate $^{231}Pa/^{230}Th$ activity ratio of the deepest model ocean grid cells. The simulated Pa/Th ratio is represented in the colour background. The observations compiled in (van Hulten et al., 2018) and references therein are represented as circles.

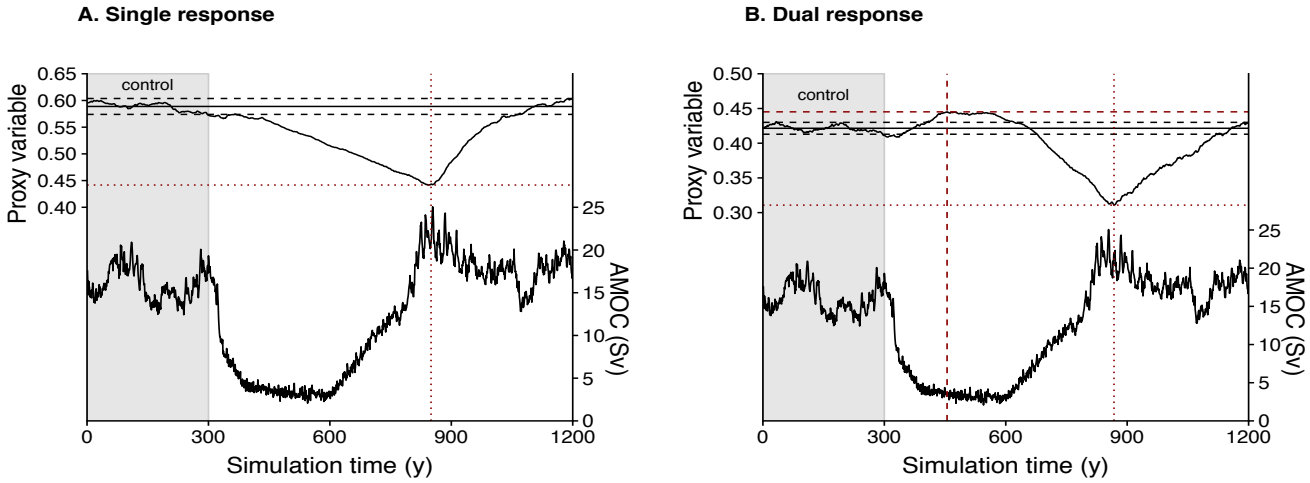

Figure 2: Theoretical definition of the proxy response studied (dotted red horizontal line) and the time of response (dotted red vertical line) in the case of A. a single response or B. a dual response to the circulation change induced by the freshwater addition. In the case of dual response, we examine the early (*i.e.* the first) and the late (*i.e.* the second) proxy response and time of response. The anomaly is defined as the difference between the proxy value at the defined time of response and the average proxy value (horizontal black line) during the control period of 300 years (highlighted in grey). The horizontal dashed black lines represent the proxy variance (2σ) over the control period (highlighted in grey). The proxy variable used is purposely not specified since the interest here is to provide an illustration of the definition used in the present study with the different modelled proxy variables.

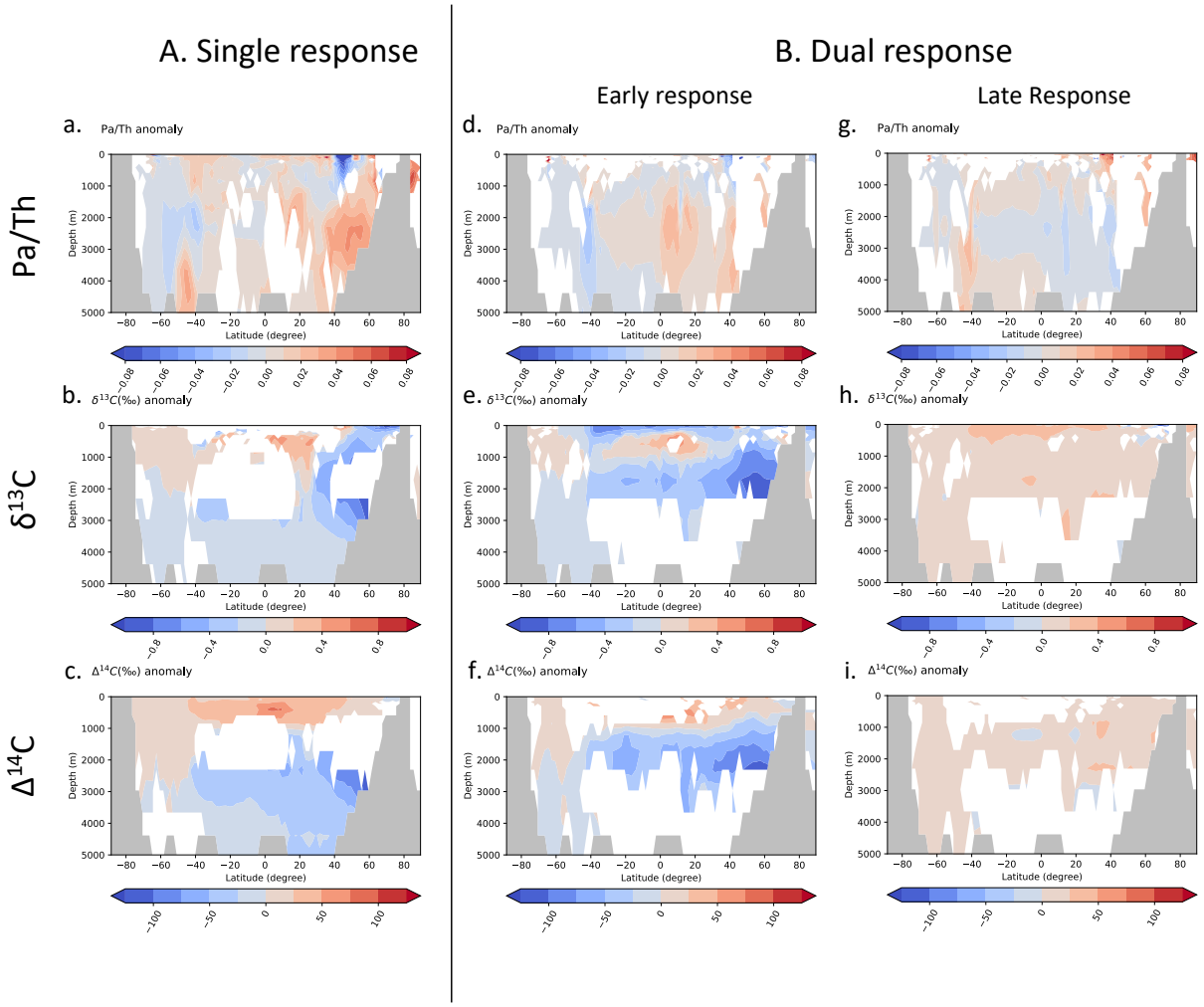

Figure 3: Zonally averaged anomalies for Pa/Th, $\delta^{13}C$ and $\Delta^{14}C$ in the western Atlantic basin in the case of a freshwater input in the Nordic seas. The western and eastern basin are delimited by the topography increase corresponding to the Mid Atlantic Ridge in the model grid. The anomalies are computed/defined as the proxy response minus the mean of the proxy value during the control period of 300 years under PI conditions (see text). **A.** (a. to c.) Represents the anomalies for the three proxies in the case where exactly one proxy response has been detected. In the case of two proxy responses, **(B.)** d.to f. represent the proxy anomaly value for the early (first) response, while g.to i. represent the proxy anomaly for the late (second) proxy response. Areas left in blank were not showing a single response (A.) or not showing exactly two responses (B.) In each subplot, the grey contours represent the ocean bottom. Single and dual responses are mutually exclusive on a per location basis. Since panels A and B are showing zonal averages, overlaps may arise from different locations with the same latitude but different longitudes.

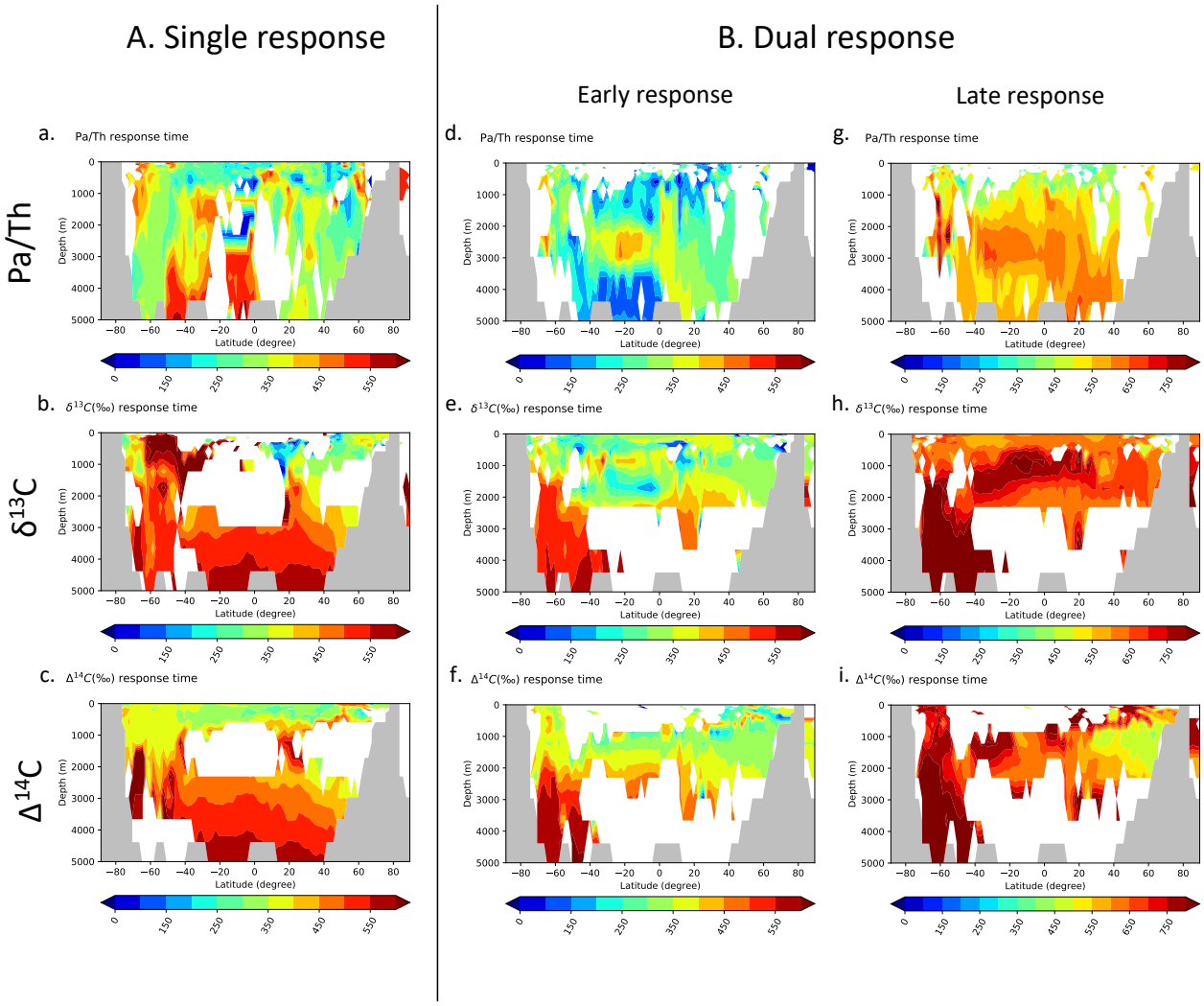

Figure 4: Zonally averaged times of response (years) for Pa/Th, $\delta^{13}C$ and $\Delta^{14}C$ in the western Atlantic basin in the case of a freshwater input in the Nordic seas. The times of response (years) correspond to the time of proxy maximal response after the beginning of freshwater addition (see text). **A.** Time of response in the case where exactly one single proxy response is detected. In the case where two distinct responses are detected **(B.)** d. to f. show the time of response of the early (first) response and g. to i. show the time of response corresponding to the late (second) response. Areas left in blank were not showing a single response (A.) or not showing exactly two responses (B.) In each subplot, the grey contours represent the ocean bottom.

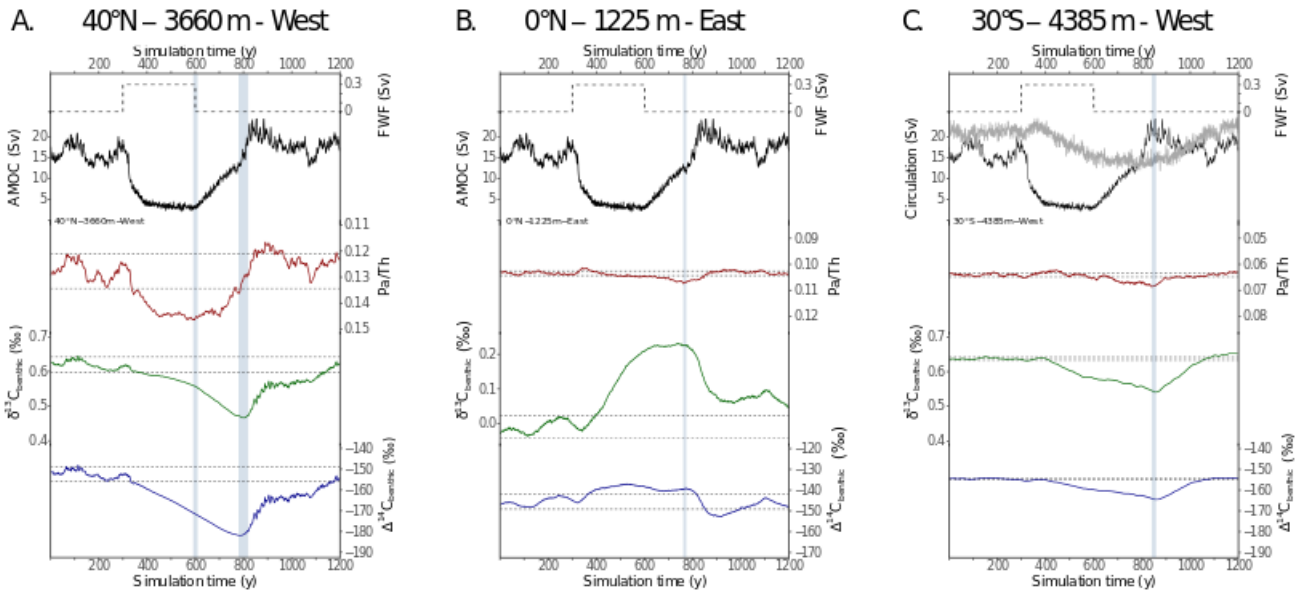

Figure 5: Selected multi-proxy time series for the Nordic Seas hosing experiment representing the three main Atlantic water masses. **A.** Zonally averaged on the western Atlantic basin time series at 40°N 3660 m. This time series is representative of the proxy behaviors in the NADW. **B.** Zonally averaged on the eastern Atlantic basin time series at 0°N 1225 m. This time series is representative of the intermediate waters. **C.** Zonally averaged on the western Atlantic basin time series at 30°S 4385 m. This time series is representative of the proxy response in the AABW. In the eastern basin, the $\delta^{13}C$ generally displays 2 responses, first increasing (not shown) and then decreasing (as shown). In each subplot from top to bottom the dashed black line represent the freshwater flux (FWF) applied in the Nordic Seas, the black line represents the North Atlantic Maximum stream function (A. B. C.), the grey line represents the Southern Ocean maximum stream function (C.), the red line represents the particulate Pa/Th, the green line represents the $\delta^{13}C$ and the blue line represents the $\Delta^{14}C$. The thin dashed black lines represent the proxy variance (2 σ) on the first 300 simulated years. The blue vertical bands indicate the timing of the proxy responses.

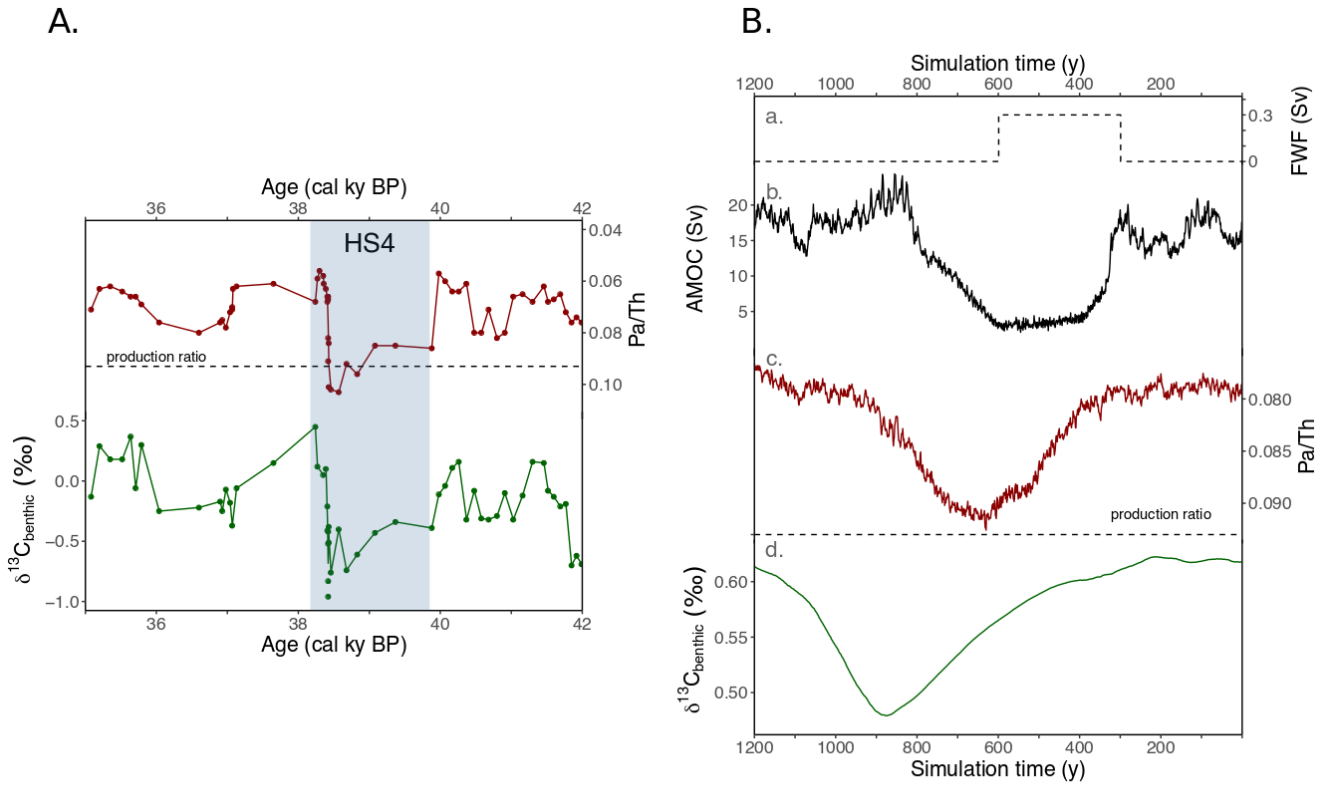

Figure 6: Example of the Bermuda Rise time series A. Pa/Th and benthic $\delta^{13}C$ (‰) measured at the Bermuda Rise around HS4 (Henry et al., 2016). **B.** Modelled time series corresponding to the average of the 9 grid cells surrounding the model grid cell closest to the Bermuda Rise (34°N-58°W). a. Imposed freshwater flux, b. Maximum North-Atlantic meridional Stream function (Sv) c. simulated Pa/Th and, d. benthic $\delta^{13}C$ (‰).

Code and data availability. The iLOVECLIM source code is based on the LOVECLIM model version 1.2 whose code is accessible at http://www.elic.ucl.ac.be/modx/elic/index.php?id=289. The developments on the iLOVECLIM source code are hosted at https://forge.ipsl.jussieu.fr/ludus but are not publicly available due to copyright restrictions. Access can be granted on demand by request to D. M. Roche (didier.roche@lsce.ipsl.fr)
The model output related to this article is available on Pangaea (https://doi.pangaea.de/10.1594/PANGAEA.900617).

Supplement. The supplement related to this article is available online.

Author contributions. LM, CW and DMR designed the research. LM, DMR, NB, JCD and AQ developed the iLOVECLIM model. LM performed the simulations. LM and JYP developed the post-processing algorithm. JCD and SP contributed to expert knowledge on Pa/Th. LM wrote the manuscript with the inputs form all the co-authors.

Competing interests. The authors declare that they have no conflict of interests.

Acknowledgements This is a contribution to ERC project ACCLIMATE; the research leading to these results has received funding from the European Research Council under the European Union's Seventh Framework Programme (FP7/2007-2013)/ERC grant agreement 339108. LM acknowledges funding from the Australian Research Council grant DP180100048. We thank S. Moreira and F. Lhardy for their help with Python. E. Michel is thanked for expert knowledge discussion on ^{14}C. This is a LSCE contribution 6949.

References

Adkins, J. F. and Boyle, E. A.: Changing atmospheric Δ14C and the record of deep water paleoventilation ages, Paleoceanography, 12(3), 337–344, doi:10.1029/97PA00379, 1997.

Alley, R. B., Sowers, T., Mayewski, P. A., Stuiver, M., Taylor, K. C. and Clark, P. U.: Holocene climatic instability: A prominent, widespread event 8200 yr ago, Geology, 25(6), 483–486, doi:10.1130/0091-7613(1997)025<0483:HCIAPW>2.3.CO;2, 1997.

Anderson, R. F., Bacon, M. P. and Brewer, P. G.: Removal of 230Th and 231Pa at ocean margins, Earth and Planetary Science Letters, 66, 73–90, doi:10.1016/0012-821X(83)90127-9, 1983.

Bard, E., Arnold, M., Mangerud, J., Paterne, M., Labeyrie, L., Duprat, J., Mélières, M.-A., Sønstegaard, E. and Duplessy, J.-C.: The North Atlantic atmosphere-sea surface 14C gradient during the Younger Dryas climatic event, Earth and Planetary Science Letters, 126(4), 275–287, doi:10.1016/0012-821X(94)90112-0, 1994.

Barker, S., Chen, J., Gong, X., Jonkers, L., Knorr, G. and Thornalley, D.: Icebergs not the trigger for North Atlantic cold events, Nature, 520, 333, 2015.

Böhm, E., Lippold, J., Gutjahr, M., Frank, M., Blaser, P., Antz, B., Fohlmeister, J., Frank, N., Andersen, M. B. and Deininger, M.: Strong and deep Atlantic meridional overturning circulation during the last glacial cycle, Nature, 517, 73, 2015.

Bondevik, S., Mangerud, J., Birks, H. H., Gulliksen, S. and Reimer, P.: Changes in North Atlantic Radiocarbon Reservoir Ages During the Allerød and Younger Dryas, Science, 312(5779), 1514, doi:10.1126/science.1123300, 2006.

Bouttes, N., Roche, D. M., Mariotti, V. and Bopp, L.: Including an ocean carbon cycle model into iLOVECLIM (v1.0), Geosci. Model Dev., 8(5), 1563–1576, doi:10.5194/gmd-8-1563-2015, 2015.

Broecker, W. S.: Massive iceberg discharges as triggers for global climate change, Nature, 372(6505), 421–424, doi:10.1038/372421a0, 1994.

Broecker, W. S., Bond, G., Klas, M., Bonani, G. and Wolfli, W.: A salt oscillator in the glacial Atlantic? 1. The concept, Paleoceanography, 5(4), 469–477, doi:10.1029/PA005i004p00469, 1990.

Brovkin, V., Ganopolski, A. and Svirezhev, Y.: A continuous climate-vegetation classification for use in climate-biosphere studies, Ecological Modelling, 101(2), 251–261, doi:10.1016/S0304-3800(97)00049-5, 1997.

Brovkin, V., Bendtsen, J., Claussen, M., Ganopolski, A., Kubatzki, C., Petoukhov, V. and Andreev, A.: Carbon cycle, vegetation, and climate dynamics in the Holocene: Experiments with the CLIMBER-2 model, Global Biogeochemical Cycles, 16(4), 86–1, doi:10.1029/2001GB001662, 2002.

Burckel, P., Waelbroeck, C., Gherardi, J. M., Pichat, S., Arz, H., Lippold, J., Dokken, T. and Thil, F.: Atlantic Ocean circulation changes preceded millennial tropical South America rainfall events during the last glacial, Geophysical Research Letters, 42(2), 411–418, doi:10.1002/2014GL062512, 2015.

Burckel, P., Waelbroeck, C., Luo, Y., Roche, D. M., Pichat, S., Jaccard, S. L., Gherardi, J., Govin, A., Lippold, J. and Thil, F.: Changes in the geometry and strength of the Atlantic meridional overturning circulation during the last glacial (20–50 ka),

Clim. Past, 12(11), 2061–2075, doi:10.5194/cp-12-2061-2016, 2016.

Butzin, M., Prange, M. and Lohmann, G.: Radiocarbon simulations for the glacial ocean: The effects of wind stress, Southern Ocean sea ice and Heinrich events, Earth and Planetary Science Letters, 235(1), 45–61, doi:10.1016/j.epsl.2005.03.003, 2005.

Chase, Z., Anderson, R. F., Fleisher, M. Q. and Kubik, P. W.: The influence of particle composition and particle flux on scavenging of Th, Pa and Be in the ocean, Earth and Planetary Science Letters, 204(1), 215–229, doi:10.1016/S0012-821X(02)00984-6, 2002.

Chase, Z., Anderson, R. F., Fleisher, M. Q. and Kubik, P. W.: Scavenging of 230Th, 231Pa and 10Be in the Southern Ocean (SW Pacific sector): the importance of particle flux, particle composition and advection, Deep Sea Research Part II: Topical Studies in Oceanography, 50(3), 739–768, doi:10.1016/S0967-0645(02)00593-3, 2003.

Chen, T., Robinson, L. F., Burke, A., Southon, J., Spooner, P., Morris, P. J. and Ng, H. C.: Synchronous centennial abrupt events in the ocean and atmosphere during the last deglaciation, Science, 349(6255), 1537, doi:10.1126/science.aac6159, 2015.

Duplessy, J. C., Shackleton, N. J., Fairbanks, R. G., Labeyrie, L., Oppo, D. and Kallel, N.: Deepwater source variations during the last climatic cycle and their impact on the global deepwater circulation, Paleoceanography, 3(3), 343–360, doi:10.1029/PA003i003p00343, 1988.

Dutay, J.-C., Lacan, F., Roy-Barman, M. and Bopp, L.: Influence of particle size and type on 231Pa and 230Th simulation with a global coupled biogeochemical-ocean general circulation model: A first approach, Geochemistry, Geophysics, Geosystems, 10(1), 2009.

Eide, M., Olsen, A., Ninnemann, U. S. and Johannessen, T.: A global ocean climatology of preindustrial and modern ocean δ13C, Global Biogeochemical Cycles, 31(3), 515–534, doi:10.1002/2016GB005473, 2017.

François, R.: Paleoflux and paleocirculation from sediment 230Th and 231Pa/230Th. Proxies in Late Cenozoic Paleoceanography, Elsevier, Amsterdam., 2007.

Friedlingstein, P., Cox, P., Betts, R., Bopp, L., von Bloh, W., Brovkin, V., Cadule, P., Doney, S., Eby, M. and Fung, I.: Climate–carbon cycle feedback analysis: results from the C4MIP model intercomparison, Journal of climate, 19(14), 3337–3353, 2006.

Gardner, W. D., Richardson, M. J. and Mishonov, A. V.: Global assessment of benthic nepheloid layers and linkage with upper ocean dynamics, Earth and Planetary Science Letters, 482, 126–134, 2018.

Gherardi, J.-M., Labeyrie, L., McManus, J. F., Francois, R., Skinner, L. C. and Cortijo, E.: Evidence from the Northeastern Atlantic basin for variability in the rate of the meridional overturning circulation through the last deglaciation, Earth and Planetary Science Letters, 240(3), 710–723, doi:10.1016/j.epsl.2005.09.061, 2005.

Godwin, H.: Half-life of radiocarbon, Nature, 195(4845), 984, 1962.

Goosse, H., Brovkin, V., Fichefet, T., Haarsma, R., Huybrechts, P., Jongma, J., Mouchet, A., Selten, F., Barriat, P.-Y., Campin, J.-M., Deleersnijder, E., Driesschaert, E., Goelzer, H., Janssens, I., Loutre, M.-F., Morales Maqueda, M. A., Opsteegh, T., Mathieu, P.-P., Munhoven, G., Pettersson, E. J., Renssen, H., Roche, D. M., Schaeffer, M., Tartinville, B., Timmermann, A. and Weber, S. L.: Description of the Earth system model of intermediate complexity LOVECLIM version 1.2, Geosci. Model

Dev., 3(2), 603–633, doi:10.5194/gmd-3-603-2010, 2010.

Gu, S. and Liu, Z.: 231 Pa and 230 Th in the ocean model of the Community Earth System Model (CESM1. 3)., Geoscientific Model Development, 10(12), 2017.

Hayes, C. T., Anderson, R. F., Fleisher, M. Q., Vivancos, S. M., Lam, P. J., Ohnemus, D. C., Huang, K.-F., Robinson, L. F., Lu, Y., Cheng, H., Edwards, R. L. and Moran, S. B.: Intensity of Th and Pa scavenging partitioned by particle chemistry in the North Atlantic Ocean, Marine Chemistry, 170, 49–60, doi:10.1016/j.marchem.2015.01.006, 2015.

Hemming, S. R.: Heinrich events: Massive late Pleistocene detritus layers of the North Atlantic and their global climate imprint, Reviews of Geophysics, 42(1), 2004.

Henderson, G. M. and Anderson, R. F.: The U-series toolbox for paleoceanography, Reviews in Mineralogy and Geochemistry, 52(1), 493–531, 2003.

Henry, L. G., McManus, J. F., Curry, W. B., Roberts, N. L., Piotrowski, A. M. and Keigwin, L. D.: North Atlantic ocean circulation and abrupt climate change during the last glaciation, Science, 353(6298), 470–474, 2016.

Hoffman, J. S., Carlson, A. E., Winsor, K., Klinkhammer, G. P., LeGrande, A. N., Andrews, J. T. and Strasser, J. C.: Linking the 8.2 ka event and its freshwater forcing in the Labrador Sea, Geophysical Research Letters, 39(18), 2012.

van Hulten, M., Dutay, J.-C. and Roy-Barman, M.: A global scavenging and circulation ocean model of thorium-230 and protactinium-231 with improved particle dynamics (NEMO–ProThorP 0.1), Geosci. Model Dev., 11(9), 3537–3556, doi:10.5194/gmd-11-3537-2018, 2018.

Kageyama, M., Merkel, U., Otto-Bliesner, B., Prange, M., Abe-Ouchi, A., Lohmann, G., Ohgaito, R., Roche, D. M., Singarayer, J. and Swingedouw, D.: Climatic impacts of fresh water hosing under Last Glacial Maximum conditions: a multi-model study, Climate of the Past, 9(2), 935–953, 2013.

Kindler, P., Guillevic, M., Baumgartner, M., Schwander, J., Landais, A. and Leuenberger, M.: Temperature reconstruction from 10 to 120 kyr b2k from the NGRIP ice core, Clim. Past, 10(2), 887–902, doi:10.5194/cp-10-887-2014, 2014.

Kleiven, H. (Kikki) F., Kissel, C., Laj, C., Ninnemann, U. S., Richter, T. O. and Cortijo, E.: Reduced North Atlantic Deep Water Coeval with the Glacial Lake Agassiz Freshwater Outburst, Science, 319(5859), 60, doi:10.1126/science.1148924, 2008.

Kretschmer, S., Geibert, W., Rutgers van der Loeff, M. M. and Mollenhauer, G.: Grain size effects on 230Thxs inventories in opal-rich and carbonate-rich marine sediments, Earth and Planetary Science Letters, 294(1), 131–142, doi:10.1016/j.epsl.2010.03.021, 2010.

Lippold, J., Grützner, J., Winter, D., Lahaye, Y., Mangini, A. and Christl, M.: Does sedimentary 231Pa/230Th from the Bermuda Rise monitor past Atlantic Meridional Overturning Circulation?, Geophysical Research Letters, 36(12), doi:10.1029/2009GL038068, 2009.

Lund, D. C., Tessin, A. C., Hoffman, J. L. and Schmittner, A.: Southwest Atlantic water mass evolution during the last deglaciation, Paleoceanography, 30(5), 477–494, doi:10.1002/2014PA002657, 2015.

Luo, Y., Francois, R. and Allen, S. E.: Sediment 231Pa/230Th as a recorder of the rate of the Atlantic meridional overturning

circulation: insights from a 2-D model., Ocean Science Discussions, 6(4), 2755–2829 [online] Available from: https://login.wwwproxy1.library.unsw.edu.au/login?url=http://search.ebscohost.com/login.aspx?direct=true&db=eih&AN=55466861&site=ehost-live&scope=site, 2010.

Lynch-Stieglitz, J.: The Atlantic Meridional Overturning Circulation and Abrupt Climate Change, Annu. Rev. Mar. Sci., 9(1), 83–104, doi:10.1146/annurev-marine-010816-060415, 2017.

Lynch-Stieglitz, J., Schmidt, M. W., Gene Henry, L., Curry, W. B., Skinner, L. C., Mulitza, S., Zhang, R. and Chang, P.: Muted change in Atlantic overturning circulation over some glacial-aged Heinrich events, Nature Geoscience, 7, 144, 2014.

Marchal, O., François, R., Stocker, T. F. and Joos, F.: Ocean thermohaline circulation and sedimentary 231Pa/230Th ratio, Paleoceanography, 15(6), 625–641, doi:10.1029/2000PA000496, 2000.

Mariotti, V., Bopp, L., Tagliabue, A., Kageyama, M. and Swingedouw, D.: Marine productivity response to Heinrich events: a model-data comparison, Climate of the Past, 8(5), 1581–1598, 2012.

McManus, J. F., Francois, R., Gherardi, J.-M., Keigwin, L. D. and Brown-Leger, S.: Collapse and rapid resumption of Atlantic meridional circulation linked to deglacial climate changes, Nature, 428(6985), 834–837, doi:10.1038/nature02494, 2004.

Menviel, L., Timmermann, A., Mouchet, A. and Timm, O.: Meridional reorganizations of marine and terrestrial productivity during Heinrich events, Paleoceanography, 23(1), doi:10.1029/2007PA001445, 2008.

Menviel, L., Mouchet, A., Meissner, K. J., Joos, F. and England, M. H.: Impact of oceanic circulation changes on atmospheric δ13CO2, Global Biogeochemical Cycles, 29(11), 1944–1961, doi:10.1002/2015GB005207, 2015.

Menviel, L., Yu, J., Joos, F., Mouchet, A., Meissner, K. J. and England, M. H.: Poorly ventilated deep ocean at the Last Glacial Maximum inferred from carbon isotopes: A data-model comparison study, Paleoceanography, 32(1), 2–17, doi:10.1002/2016PA003024, 2017.

Missiaen, L., Pichat, S., Waelbroeck, C., Douville, E., Bordier, L., Dapoigny, A., Thil, F., Foliot, L. and Wacker, L.: Downcore Variations of Sedimentary Detrital (238U/232Th) Ratio: Implications on the Use of 230Thxs and 231Paxs to Reconstruct Sediment Flux and Ocean Circulation, Geochemistry, Geophysics, Geosystems, 19(8), 2560–2573, doi:10.1029/2017GC007410, 2018.

Mulitza, S., Chiessi, C. M., Schefuß, E., Lippold, J., Wichmann, D., Antz, B., Mackensen, A., Paul, A., Prange, M., Rehfeld, K., Werner, M., Bickert, T., Frank, N., Kuhnert, H., Lynch-Stieglitz, J., Portilho-Ramos, R. C., Sawakuchi, A. O., Schulz, M., Schwenk, T., Tiedemann, R., Vahlenkamp, M. and Zhang, Y.: Synchronous and proportional deglacial changes in Atlantic meridional overturning and northeast Brazilian precipitation, Paleoceanography, 32(6), 622–633, doi:10.1002/2017PA003084, 2017.

Ng, H. C., Robinson, L. F., McManus, J. F., Mohamed, K. J., Jacobel, A. W., Ivanovic, R. F., Gregoire, L. J. and Chen, T.: Coherent deglacial changes in western Atlantic Ocean circulation, Nature Communications, 9(1), 2947, doi:10.1038/s41467-018-05312-3, 2018.

Orr, J. C., Maier-Reimer, E., Mikolajewicz, U., Monfray, P., Sarmiento, J. L., Toggweiler, J. R., Taylor, N. K., Palmer, J., Gruber, N., Sabine, C. L., Le Quéré, C., Key, R. M. and Boutin, J.: Estimates of anthropogenic carbon uptake from four three-

dimensional global ocean models, Global Biogeochemical Cycles, 15(1), 43–60, doi:10.1029/2000GB001273, 2001.

Rempfer, J., Stocker, T. F., Joos, F., Lippold, J. and Jaccard, S. L.: New insights into cycling of 231Pa and 230Th in the Atlantic Ocean, Earth and Planetary Science Letters, 468, 27–37, doi:10.1016/j.epsl.2017.03.027, 2017.

Roche, D. M., Wiersma, A. P. and Renssen, H.: A systematic study of the impact of freshwater pulses with respect to different geographical locations, Climate Dynamics, 34(7), 997–1013, doi:10.1007/s00382-009-0578-8, 2010.

Schlitzer, R., Anderson, R. F., Dodas, E. M., Lohan, M., Geibert, W., Tagliabue, A., Bowie, A., Jeandel, C., Maldonado, M. T. and Landing, W. M.: The GEOTRACES intermediate data product 2017, Chemical Geology, 493, 210–223, 2018.

Schmittner, A. and Lund, D. C.: Early deglacial Atlantic overturning decline and its role in atmospheric CO2 rise inferred from carbon isotopes (δ13C), Clim. Past, 11(2), 135–152, doi:10.5194/cp-11-135-2015, 2015.

Schmittner, A. B.: Impact of the Ocean's Overturning Circulation on Atmospheric CO2, American Geophysical Union., 2007.

Siddall, M., Henderson, G. M., Edwards, N. R., Frank, M., Müller, S. A., Stocker, T. F. and Joos, F.: 231Pa/230Th fractionation by ocean transport, biogenic particle flux and particle type, Earth and Planetary Science Letters, 237(1), 135–155, doi:10.1016/j.epsl.2005.05.031, 2005.

Siddall, M., Stocker, T. F., Henderson, G. M., Joos, F., Frank, M., Edwards, N. R., Ritz, S. P. and Müller, S. A.: Modeling the relationship between 231Pa/230Th distribution in North Atlantic sediment and Atlantic meridional overturning circulation, Paleoceanography, 22(2), doi:10.1029/2006PA001358, 2007.

Siegenthaler, U. and Münnich, K. O.: C/12 C fractionation during CO 2 transfer from air to sea, Carbon Cycle Modelling. Bolin B.(ed) Wiley, New York, 249–257, 1981.

Skinner, L. C. and Shackleton, N. J.: Rapid transient changes in northeast Atlantic deep water ventilation age across Termination I, Paleoceanography, 19(2), doi:10.1029/2003PA000983, 2004.

Skinner, L. C., Waelbroeck, C., Scrivner, A. E. and Fallon, S. J.: Radiocarbon evidence for alternating northern and southern sources of ventilation of the deep Atlantic carbon pool during the last deglaciation, Proc Natl Acad Sci USA, 111(15), 5480, doi:10.1073/pnas.1400668111, 2014.

Smeed, D. A., McCarthy, G. D., Cunningham, S. A., Frajka-Williams, E., Rayner, D., Johns, W. E., Meinen, C. S., Baringer, M. O., Moat, B. I., Duchez, A. and Bryden, H. L.: Observed decline of the Atlantic meridional overturning circulation 2004–2012, Ocean Sci., 10(1), 29–38, doi:10.5194/os-10-29-2014, 2014.

Stanford, J. D., Rohling, E. J., Bacon, S., Roberts, A. P., Grousset, F. E. and Bolshaw, M.: A new concept for the paleoceanographic evolution of Heinrich event 1 in the North Atlantic, Quaternary Science Reviews, 30(9), 1047–1066, doi:10.1016/j.quascirev.2011.02.003, 2011.

Stuiver, M. and Polach, H. A.: Discussion Reporting of 14C Data, Radiocarbon, 19(3), 355–363, doi:10.1017/S0033822200003672, 1977.

Tessin, A. C. and Lund, D. C.: Isotopically depleted carbon in the mid-depth South Atlantic during the last deglaciation, Paleoceanography, 28(2), 296–306, doi:10.1002/palo.20026, 2013.

Thomas, A. L., Henderson, G. M. and Robinson, L. F.: Interpretation of the 231Pa/230Th paleocirculation proxy: New water-

column measurements from the southwest Indian Ocean, Earth and Planetary Science Letters, 241(3), 493–504, doi:10.1016/j.epsl.2005.11.031, 2006.

Thomson, J., Colley, S., Anderson, R., Cook, G. T., MacKenzie, A. B. and Harkness, D. D.: Holocene sediment fluxes in the northeast Atlantic from 230Thexcess and radiocarbon measurements, Paleoceanography, 8(5), 631–650, doi:10.1029/93PA01366, 1993.

Thornalley, D. J. R., Barker, S., Broecker, W. S., Elderfield, H. and McCave, I. N.: The Deglacial Evolution of North Atlantic Deep Convection, Science, 331(6014), 202, doi:10.1126/science.1196812, 2011.

Thornalley, D. J. R., Bauch, H. A., Gebbie, G., Guo, W., Ziegler, M., Bernasconi, S. M., Barker, S., Skinner, L. C. and Yu, J.: A warm and poorly ventilated deep Arctic Mediterranean during the last glacial period, Science, 349(6249), 706, doi:10.1126/science.aaa9554, 2015.

Tschumi, T., Joos, F., Gehlen, M. and Heinze, C.: Deep ocean ventilation, carbon isotopes, marine sedimentation and the deglacial CO2 rise, Clim. Past, 7(3), 771–800, doi:10.5194/cp-7-771-2011, 2011.

Waelbroeck, C., Duplessy, J.-C., Michel, E., Labeyrie, L., Paillard, D. and Duprat, J.: The timing of the last deglaciation in North Atlantic climate records, Nature, 412(6848), 724–727, doi:10.1038/35089060, 2001.

Waelbroeck, C., Pichat, S., Böhm, E., Lougheed, B. C., Faranda, D., Vrac, M., Missiaen, L., Vazquez Riveiros, N., Burckel, P., Lippold, J., Arz, H. W., Dokken, T., Thil, F. and Dapoigny, A.: Relative timing of precipitation and ocean circulation changes in the western equatorial Atlantic over the last 45 kyr, Clim. Past, 14(9), 1315–1330, doi:10.5194/cp-14-1315-2018, 2018.

Wheatcroft, R. A.: Experimental tests for particle size-dependent bioturbation in the deep ocean, Limnology and Oceanography, 37(1), 90–104, doi:10.4319/lo.1992.37.1.0090, 1992.

Wiersma, A. P. and Renssen, H.: Model–data comparison for the 8.2kaBP event: confirmation of a forcing mechanism by catastrophic drainage of Laurentide Lakes, Quaternary Science Reviews, 25(1), 63–88, doi:10.1016/j.quascirev.2005.07.009, 2006.

Yu, E.-F., Francois, R. and Bacon, M. P.: Similar rates of modern and last-glacial ocean thermohaline circulation inferred from radiochemical data, Nature, 379(6567), 689–694, doi:10.1038/379689a0, 1996.

Zhao, N., Marchal, O., Keigwin, L., Amrhein, D. and Gebbie, G.: A Synthesis of Deglacial Deep-Sea Radiocarbon Records and Their (In)Consistency With Modern Ocean Ventilation, Paleoceanography and Paleoclimatology, 33(2), 128–151, doi:10.1002/2017PA003174, 2018.

Table 1: Parameters used in the Pa/Th module

Symbol	Variable	Value	Units
j	^{231}Pa or ^{230}Th	-	-
i	Particle type ($CaCO_3$, POC, opal)	-	-
A_p^j	Particle-bound activity	Calculated – see Eq. 2.	$dpm.m^{-3}.y^{-1}$
A_d^j	Dissolved activity	Calculated – see Eq. 1.	$dpm.m^{-3}.y^{-1}$
β^{Pa}	Production of ^{231}Pa from U-decay	$2.33\ 10^{-3}$	$dpm.m^{-3}.y^{-1}$
β^{Th}	Production of ^{230}Th from - decay	$2.52\ 10^{-2}$	$dpm.m^{-3}.y^{-1}$
λ_{Pa}	Decay constant for ^{231}Pa	$2.116\ 10^{-5}$	y^{-1}
λ_{Th}	Decay constant for ^{230}Th	$9.195\ 10^{-6}$	y^{-1}
K_{adsorp}^j	Adsorption coefficient	Calculated – see Eq. 3.	y^{-1}
k_{desorp}	Desorption coefficient	2.4	y^{-1}
$\sigma_{i,j}$	Scavenging efficiency	See Table 2	$m^2.mol^{-1}$
F_i	Particle flux	Calculated in each grid cell $Fi = [particle\ conc].\ w_s$	$mol.m^{-2}.y^{-1}$
w_s	Uniform settling speed	1,000	$m.y^{-1}$

Table 2: Best fit $\sigma_{i,j}$ values and corresponding Kd values

	$\sigma_{Pa\text{-}CaCO3}$	$\sigma_{Pa\text{-}POC}$	$\sigma_{Pa\text{-}opal}$	$\sigma_{Th\text{-}CaCO3}$	$\sigma_{Th\text{-}POC}$	$\sigma_{Th\text{-}opal}$
Best fit	1.87	1.55	7.62	76.83	5.47	3.77
	$Kd_{Pa\text{-}CaCO3}$	$Kd_{Pa\text{-}POC}$	$Kd_{Pa\text{-}opal}$	$Kd_{Th\text{-}CaCO3}$	$Kd_{Th\text{-}POC}$	$Kd_{Th\text{-}opal}$
Best fit	8.01E+06	5.53E+07	4.86E+07	3.29E+08	1.96E+08	2.40E+07

Carbon isotopes and Pa/Th response to forced circulation changes: a model perspective

Note to the Editor and referees

We have requested a long deadline extension since a bug was found in the iLOVECLIM model code that could affect the carbon cycle part. To ensure scientific reproducibility, we first wanted to assess whether the bug found could have a significant impact on our results. This has required to run several multi-millennial long simulations. After analysis of the results of the newer version, we however found that our conclusions are unaffected by this error. We thank the Editor and the referees for their patience in this necessary process.

Response to the referees' comments

We thank both reviewers for their constructive comments that helped to improve and clarify the manuscript. We have addressed the comments in detail below.

Anonymous Referee #2

This is a report on the implementation of the Pa/Th sedimentary proxy in the ocean-climate model of intermediate complexity, iLOVECLIM, in addition to the previously included stable carbon and radiocarbon isotope ratios. The reconstruction of past circulation states has suggested substantial changes from that observed in the modern ocean, with potentially significant implications for past climate change. It is therefore important that model simulations can capture the observed sedimentary evidence and demonstrate the ocean physics that might be consistent with this evidence. In this case, the incorporation of multiple isotopic tracers with different distribution and influences adds a valuable layer of sophistication to such modeling efforts.

In addition to demonstrating the model's ability to reproduce the observed modern distributions of Pa/Th and carbon isotopes, the authors report on the results of what is now a relatively standard "hosing" experiment, wherein freshwater is imposed on the surface of the high latitude North Atlantic within the model domain, in order to weaken convection and the overturning circulation. Changes in subsurface water masses and the strength of the overturning have the result of redistributing the sedimentary Pa/Th and carbon isotopes, which the authors then interpret and compare to existing data. They identify different responses of in the respective tracers. One major finding is that in the hosing experiment, changes in both carbon isotopes lag Pa/Th by a few hundred years.

Overall, this study is an important step forward in terms of the state of the art of implementation of circulation proxies and should therefore be worth accepting for publication in Climate of the Past, following revisions that should address the following points.

Carbon isotopes and Pa/Th response to forced circulation changes: a model perspective

Note to the Editor and referees

We have requested a long deadline extension since a bug was found in the iLOVECLIM model code that could affect the carbon cycle part. To ensure scientific reproducibility, we first wanted to assess whether the bug found could have a significant impact on our results. This has required to run several multi-millennial long simulations. After analysis of the results of the newer version, we however found that our conclusions are unaffected by this error. We thank the Editor and the referees for their patience in this necessary process.

Response to the referees' comments

We thank both reviewers for their constructive comments that helped to improve and clarify the manuscript. We have addressed the comments in detail below.

Anonymous Referee #1

The authors implement Pa/Th in the intermediate complexity model LOVECLIM. With the carbon isotopes, which are already in the model, the authors evaluate the responses of different proxies to the freshwater fluxes in the North Atlantic in a classical hosing experiment. They find that the Pa/Th leads the carbon isotopes by a few hundred years in the deep Atlantic. Pa/Th has been implemented in different GCMS and the authors follow the approach in Rempfer et al. (2017). Also, modeled Pa/Th response to fresh water fluxes added to the North Atlantic is carried out in previous studies (Gu and Liu, 2017; Rempfer et al., 2017). However, the comparison between Pa/Th and carbon isotopes helps to distinguish this study with previous modeling studies. Revisions are needed before this could be acceptable for publication.

Major Comments:

1. I find the separation of the single response and the dual response quite confusing. First, is it really to identify the responses this way? It seems that for the dual response, the first response is associated with the AMOC reduction and the second response is associated with the AMOC overshoot (as pointed out in page 6 line 30). I think it is easier for people to follow if you state this as a response to decreased AMOC or increased AMOC instead of first or late response. Secondly, why some grids (for example 40S, 4000m, Figure 3 a, d and g) show both single response and dual response?

We thank the reviewer for highlighting the importance of the chosen terminology. We agree with the reviewer, in numerous locations, the "first response" seems to be associated with the AMOC reduction and the "the second response" with the AMOC

overshoot. However, this is **not always true**. For instance, as pointed out in the manuscript, some locations display more than 2 responses, highlighting the complexity of identifying the proxy response to the AMOC slowdown or overshoot. Furthermore, for grid cells displaying strictly two responses, the first response does not necessarily correspond to the expected response to the AMOC slowdown. For instance, Figure 2B actually shows a $\delta_{13}C$ time series that displays a $\delta_{13}C$ increase as first response and a $\delta_{13}C$ decrease as a "second" or late response. In this case the first response likely corresponds to an accumulation of nutrients due to the cessation of NADW export as suggested in (Menviel et al., 2015) while the second or late response corresponds to the expected $\delta_{13}C$ decrease subsequent of an AMOC slowdown. Therefore, we kept the terminology of "first" and "second" response throughout the manuscript.

The second point of this comment on Figure 3 has also been raised by the reviewer #2 (see response to reviewer #2 comments). We agree with both reviewers; single and dual responses are clearly **mutually exclusive**. However, Figure 3 shows **zonally averaged** proxy responses over the western Atlantic. Consequently, for one grid cell to appear blank on Figure 3 A. (resp. 3.B.) it is required that the zonal average is empty and consequently that there is no grid cell in the full longitude range considered displaying a single response (resp. dual response). Therefore, it is possible to have overlaps on Figure 3. We added a sentence to Figure 3's caption in order to clarify this point:

"Single and dual responses are mutually exclusive on a per location basis. Since panels A and B are showing zonal averages, overlaps may arise from different locations with the same latitude but different longitudes."

2. Responses of Pa/Th and carbon isotopes in the Atlantic in a hosing experiment are not new and have been examined in other studies already. Since this paper focuses on Pa/Th, their modeled Pa/Th response should be compared to previous studies (Gu and Liu, 2017; Rempfer et al., 2017). Spatial and temporal similarities and differences with these previous studies should be compared and discussed.

We thank the reviewer for highlighting that the study from (Gu and Liu, 2017) dealing with Pa and Th in CESM was not cited in the original manuscript. We have now included a citation to this study in the revised manuscript.

It is true that the Pa/Th response to AMOC slowdown in hosing experiments has already been examined in different versions of Bern 3D (Rempfer et al., 2017; Siddall et al., 2007) and in CESM (Gu and Liu, 2017). We agree with the reviewer that it would be of great interest to evaluate the spatial and temporal similarities of the Pa/Th responses in those different models. This is however not an easy task and would require new coordinated modeling experiments with the different models. Indeed, the parameters of the hosing experiments performed (flux, input location and duration) are quite different in our study and in (Gu and Liu, 2017; Rempfer et al., 2017; Siddall et al., 2007). On the novelty of our study, we would like to point out that the Pa/Th response to the AMOC slowdown has not been assessed in a consistent way in the different above cited publications, most of them only displaying the Pa/Th response at selected locations of the North-Atlantic. Likewise, it is worth to point out that our study is the only one to consider spatial and temporal variability of the Pa/Th response to AMOC changes. Therefore, a detailed evaluation of spatial and temporal similarities

as requested by the reviewer is i) not achievable given the existing publications and ii) out of the scope of this manuscript which focuses on the spatial and temporal similarities and differences between 2 carbon isotopes proxies and the Pa/Th in a single model. Given the interest of the topic, we have added a paragraph in the discussion section to acknowledge that Pa/Th response to AMOC slowdown has already been studied in other models and highlight that the Pa/Th response obtained in the present study is quite consistent with what has been observed in previous studies (see revised manuscript).

3. At the end of the introduction, three questions are raised. The first two questions are discussed in section 3 and 4, but the third question "How can the modelled multi-proxy response help to interpret the paleoproxy records" is not clearly answered. The implication for interpreting the paleoproxy records is not clearly state. This is a very important question for modeling proxies in GGMS. Authors need to add some discussion about this kind of implications in the discussion.

We thank the reviewer for this point. One of the main motivations for multi-proxy modelling is to achieve a more efficient model-data comparison by bringing model output closer to the observables (the proxy records). This study is the first one considering $\delta_{13}C$, $_{14}C$ and Pa/Th in a consistent modelling frame and it shows 1) strong spatial variability in the proxy response (according to the main water mass bathing the considered locations) and 2) the possibility for a time delay between proxy responses at a given location (200 year lag of the carbon isotopes response relative to the Pa/Th response in the deep Northwest Atlantic). Therefore, our results show that the interpretation of the proxy data might be complicated because a given circulation change event does not necessarily produce a single and consistent proxy response in the entire Atlantic basin, nor a synchronous multi-proxy response at a given core location. We have now revised the entire discussion and conclusions sections of the manuscript to account for the comments that we received, and we hope the implication of our study for the interpretation of the proxy records is now clearer regarding this topic.

4. More differences between Pa/Th and carbon isotopes in reconstructing past AMOC could be discussed and highlighted. As mentioned above, the novelty of this paper is studying the Pa/Th together with carbon isotopes since the Pa/Th and carbon isotopes in a hosing experiment have been presented in previous studies. However, I feel this multi-proxy comparison is not fully developed in the current manuscript. A more in-depth comparison between Pa/Th and carbon isotopes and their implications for paleoceanography (back to comment 3) are needed.

As already mentioned previously, and further explained below in this response to the reviewers, the discussion section of the manuscript has undergone very substantial revisions. It now includes a more in depth comparison of Pa/Th and carbon isotopes as requested by the reviewer. See for example lines 27 to 40 p8.

5. Pa/Th leads carbon isotopes, but lead by how many years? From Figure 5 a and c, it seems that the 300 years hosing is too short for carbon isotopes to fully adjust to the reduction of AMOC. If hosing is kept longer than 300 years, carbon isotopes may lag Pa/Th response even longer. Therefore, from this 300-years hosing experiment, we cannot determine the exact lead time. This should be pointed out.

As shown on Figure 4, the actual response times and therefore the lag time between Pa/Th and carbon isotopes responses has a strong spatial variability (with locations showing actually no lag, as shown on Figure 5). We agree that 300 years of freshwater addition is likely too short for the carbon isotopes to fully adjust. The revised discussion section now highlights these 2 points.

6. The modeled Pa/Th is compared to observations in Dutay et al., 2009 and Henderson et al., 1999 (Page 5, line 14). However, in recent years, many new observations are now available. GEOTRACES offers a lot of relevant new data (also used in Rempfer et al., 2017). More core top Pa/Th are also available. A more complete compilation of the observations should be used to tune the model parameters. Also, if comparing to the same compilation of observations as in previous studies (Gu and Liu, 2017; Rempfer et al., 2017; Van Hulten et al., 2018), model performance in simulating Pa/Th can be estimated quantitatively.

We agree with the reviewer that the GEOTRACES intermediate data product 2017 (Schlitzer et al., 2018) offers relevant new data. In fact, the core-top data used in Figure 1 is actually the same that was compiled in (van Hulten et al., 2018). We have corrected the citations in the manuscript accordingly. Besides, we have updated the supplementary figures for the sake of a better model performance evaluation. The main and supplementary figures now display: i) the zonally averaged Atlantic dissolved and particulate Pa, Th and Pa/Th (as suggested by the reviewer #2), ii) the model-data comparison along GEOTRACES transect GA03 and GA02S as shown in (Gu and Liu, 2017; van Hulten et al., 2018; Rempfer et al., 2017). The question of assessing the model performance using the GEOTRACES data and comparison with previous studies is developed in the response to reviewer #2- major comment n°1 below.

Minor Comments: 1. Page 3, Line 27, Gu et al. (2017) simulating Pa/Th in CESM should be mentioned here (higher resolution then Rempfer et al. (2017) and longer integration than van Hulten et al. (2018)). Gu, S., Liu, Z., 2017. 231Pa and 230Th in the ocean model of the Community Earth System Model (CESM1.3). Geosci. Model Dev. 10, 4723–4742. https://doi.org/10.5194/gmd-10-4723-2017

We thank the reviewer for highlighting this relevant reference, which has been added to the text as suggested (see revised manuscript).

2. Page 4, Authors follow Rempfer et al. (2017) to implement Pa/Th. One advance in Rempfer et al. (2017) in simulating Pa/Th is that bottom scavenging and boundary scavenging are included, which improves the simulation of water column Pa and Th activity. In page 8, line 37, authors state that the bottom and boundary scavenging

are not modeled in LOVECLIM. This should be mentioned earlier in section 2.1 (model description and developments). Also, the modeling scheme (similarities and differences) comparing with previous modeling efforts should be discussed explicitly in section 2.1.

We agree with the reviewer, among the models able to simulate the evolution of the Pa and the Th, Bern 3D is the only one having an explicit parametrization for bottom and boundary scavenging. As stated by the authors, this parametrization is rather crude and consists in scaling (increasing) the Pa scavenging coefficients in the coastal grid-cells in order to achieve enhanced Pa removal at the ocean boundaries (Rempfer et al., 2017).

We would like to point out that all models actually represent the so-called boundary scavenging effect. Indeed, the particles fluxes produced by the GCM NEMO-PISCES and used in iLOVECLIM show greater fluxes at the continental margins compared to the ocean interior. Therefore, the higher particle fluxes induce a greater Pa removal in the regions of high particle fluxes, even in the absence of additional parametrization of the boundary scavenging. Therefore, the need for an additional parametrization of the boundary scavenging does not appear to be fundamental.

The scavenging scheme and modelling choices are fully described in the method section. To date, the Pa and Th have been implemented in at least 5 models of intermediate complexity or GCMs. Therefore, a full discussion of the similarities and differences between these models would represent a model intercomparison project, which is out of the scope of this paper. Nevertheless, we have followed the reviewer's recommendations and modified the method description to i) mention that no explicit parametrization of boundary and bottom scavenging have been included in iLOVECLIM and ii) add information about how the modelling scheme used in this study compares with previous Pa/Th modelling work (see the method section of the revised manuscript).

3. Page 5, Line 20 Details about the PI forcing should be provided. From Figure 5, there is interannual variability. Is the PI forcing looping in the first 300 years?

The meaning of the question from the reviewer is unclear to us. Is the question related to interannual variability in the climate model itself? The setup we are using is a fully coupled atmosphere – ocean – vegetation climate model. Within that climate model system there is some interannual variability simulated in the climate by itself. Regarding the boundary conditions of the climate model, these are fixed to pre-industrial conditions and as such, there is no looping condition. The interannual variability in the model is not a product of the boundary conditions imposed but of the interactions within the atmosphere – ocean – vegetation climate numerical system used.

4. Section 3.1 Vertical structures of Pa/Th could also be provided and compared to observations (GEOTRACES transects), such as Figure 2 and Figure 3 in Rempfer et al. 2017. Figure S1 only have particulate and dissolved Pa and Th.

We would like to highlight that (Gu and Liu, 2017; Rempfer et al., 2017) only provide dissolved Pa and Th as well as particulate Pa/Th (i.e. no particulate Pa and Th) along

the GEOTRACES transects GA03 and GA02S. As detailed above, we have included new supplementary figures showing dissolved, particulate Pa, Th and Pa/Th on a N-S Atlantic section as well as along GEOTRACES transect GA03 and GA02S (see response to previous comments and response to reviewer's 2 major comment n°1).

5. Page 6, section 3.2, first paragraph, Figure 5 can be referred here. Then people can see exactly how the fresh water is added and how the AMOC evolves.

Done

6. Page 6, line 14-16, this sentence can be rewritten for easier understanding.

We have split this sentence into two and added a coma (as suggested by the reviewer #2). We hope this technical information is now clearer.

7. Page 7, line 15, Any explanations for the 14C response time difference between the eastern and western basin?

The NADW is stronger in the western basin (western boundary current). The circulation pathways are hence different in the western and eastern Atlantic, both in real life and in the models. The NADW is less active in the eastern basin, which can explain the ^{14}C response pattern (see revised manuscript p7 L33).

8. Figure 2 gives two examples of the single response and dual response. What is the proxy exactly? Pa/Th? 13C? or 14C? And where is the grid, location and depth? Also, it would be good to add AMOC in this plot for people to follow.

We thank the reviewer for his/her comment. However, we think that the purpose of Figure 2 has been misinterpreted.

Figure 2 has for only purpose to display the theoretical definition of "proxy response" and "proxy response time" as defined in the text whatever the grid cell, actual location and water depth. What is represented is $\delta_{13}C$ but the figure would be valid for any time series for any proxy. We have included the AMOC time series in Figure 2 as suggested by the reviewer.

9. Authors use fixed particle fluxes in their hosing experiment. After adding fresh water to the North Atlantic, the particle fluxes will change. Will this particle flux change affect the results of this paper should be discussed.

We agree with the reviewer that any change of the ocean surface conditions (adding freshwater, temperature…) will likely induce particle fluxes changes (i.e. flux intensity and/or composition). In its current version, with fixed particles, iLOVECLIM does not simulate the impact of primary productivity changes on the Pa/Th. Instead, we only simulate the impact of circulation changes, which is of interest in itself. As stated above, we have revised the discussion section of the manuscript and ensured to clearly state and discuss the implication of the use of fixed and prescribed particle fluxes.

10. The conclusions and perspectives can be improved to highlight the major findings. Currently, it is too broad and descriptive.

We have rewritten the conclusion in order to highlight the major findings.

References:

Gu, S. and Liu, Z.: 231 Pa and 230 Th in the ocean model of the Community Earth System Model (CESM1. 3)., Geosci. Model Dev., 10(12), 2017.
van Hulten, M., Dutay, J. C. and Roy-Barman, M.: A global scavenging and circulation ocean model of thorium-230 and protactinium-231 with realistic particle dynamics (NEMO–ProThorP 0.1), Geosci Model Dev Discuss, 2017, 1–32, doi:10.5194/gmd-2017-274, 2018.
Menviel, L., Mouchet, A., Meissner, K. J., Joos, F. and England, M. H.: Impact of oceanic circulation changes on atmospheric δ13CO2, Glob. Biogeochem. Cycles, 29(11), 1944–1961, doi:10.1002/2015GB005207, 2015.
Rempfer, J., Stocker, T. F., Joos, F., Lippold, J. and Jaccard, S. L.: New insights into cycling of 231Pa and 230Th in the Atlantic Ocean, Earth Planet. Sci. Lett., 468, 27–37, doi:https://doi.org/10.1016/j.epsl.2017.03.027, 2017.
Schlitzer, R., Anderson, R. F., Dodas, E. M., Lohan, M., Geibert, W., Tagliabue, A., Bowie, A., Jeandel, C., Maldonado, M. T. and Landing, W. M.: The GEOTRACES intermediate data product 2017, Chem. Geol., 493, 210–223, 2018.
Siddall, M., Stocker, T. F., Henderson, G. M., Joos, F., Frank, M., Edwards, N. R., Ritz, S. P. and Müller, S. A.: Modeling the relationship between 231Pa/230Th distribution in North Atlantic sediment and Atlantic meridional overturning circulation, Paleoceanography, 22(2), doi:10.1029/2006PA001358, 2007.

A more careful data-model comparison is needed to validate the simulated Pa and Th, which is the main advance made in the model. The paper compares bottom water particulate Pa/Th with a core top compilation (Henderson et al., 1999). Other than that, the comparison with Pa/Th data is mostly qualitative. The authors acknowledge that they refrained from making more data/model comparisons because of the crudeness of the model (Page 8 Line 41 (P8L41)). However, it is still important to show those comparisons. Readers may gain information about the fidelity (or lack thereof) of the model to the modern observations, including regions where the model performs well and regions where it does not. This information will help make the audience more informed, and therefore increase the impact of the paper. For example, the paper mentions the compilations of sedimentary Pa/Th by Lippold et al. (2016) and Ng et al. (2018) (P9L6). How does the model compare with them graphically? How do the particulate and dissolved Pa and Th results compare with GEOTRACES observations? These could be addressed in a few brief passages.

The two reviews received highlighted the need for a more careful model data-comparison. We agree that it is important to show where the model performs well and where it does not. We have thus revised the corresponding set of figures (Figures S1 to S3) and text accordingly. As already mentioned, the core top compilation used in Figure 1 is actually the same compilation as presented in (van Hulten et al., 2018), we have corrected the references in the manuscript accordingly. Besides, we are now presenting the relevant modelled variables on the GEOTRACES transects GA03 and GA02S shown in previous studies (Gu and Liu, 2017; van Hulten et al., 2018; Rempfer et al., 2017) as detailed below.

Both reviewers mentioned the need of a more quantitative model evaluation. As explained in the supplementary text S1, we have calculated the RMSE of dissolved and particulate Pa and Th and noticed that while improving the Th variables, we were actually deteriorating the Pa variables and vice versa… Besides, we would like to point out that none of the previously published Pa/Th implementations really achieved a proper quantitative evaluation of the model-data agreement between model PI output and modern datasets. What is usually shown is the dissolved Pa and Th profiles along with the particulate Pa/Th on GEOTRACES transects GA03 and GA02 ((Gu and Liu, 2017; van Hulten et al., 2018; Rempfer et al., 2017)) as well as the sedimentary Pa/Th against Holocene core top data and remains a graphical and qualitative evaluation.

At this stage, and because at least 5 implementations of Pa and Th in different models of intermediate complexity and GCMs have been published so far, a quantitative model-data evaluation would make more sense in the frame of an extensive model-model and model-data intercomparison. Such a work is clearly out of the scope of this study and is the subject of ongoing work by the lead author for a subsequent publication.

In addition, we would like to highlight a few points concerning the use of the GEOTRACES data for model performance evaluation. It is clear that the GEOTRACES database provides a growing amount of data for comparison with model outputs. However, we think that it is worth to point out a few issues:

- First of all, it is worth noting that the model outputs represent averages of several years of run under equilibrium state while GEOTRACES data

correspond to one particular sampling date. Besides, depending on the model resolution, several GEOTRACES data points can correspond to one single model grid box… All in all, it seems important to us to stress that the model can sometimes display a feature "at the wrong" position, so any point by point comparison has to be handled carefully.

- What is reported in the GEOTRACES dataset (Schlitzer et al., 2018) are total dissolved or particulate ^{231}Pa and ^{230}Th activities corrected for measurement blanks and ingrowth since sample collection. These relatively "raw" concentrations do contain a signal from the ^{231}Pa and ^{230}Th coming from detrital (dissolution of terrigenous material or terrigenous component of particles) as well as ^{231}Pa and ^{230}Th coming from water column scavenging (also called excess fraction). The different fractions/contributions can be derived from the ^{231}Pa, ^{230}Th and ^{232}Th concentrations using a few assumptions and can sometimes represent more than 10% of the signal. It seems important to remind that what is actually computed by the models is solely the Pa and Th derived from the water column U-decay. Any other source of Pa and Th is not taken into account by the models. However, none of the published modelling paper mentions which concentrations (corrected or not – which correction) have been considered. This complicates the evaluation of the model performances and motivates an extensive model intercomparison. For the reasons mentioned above, using the full potential of the GEOTRACES dataset would therefore require to first determine a method for the calculation of the excess fractions as the pre-calculated excess concentrations are only available for 2 Atlantic profiles. Such work is clearly beyond the scope of the present study.

For all of the reasons explained above and for the sake of consistency with the model evaluations that have been previously published we are now showing for the model-data evaluation:

- The modelled sedimentary Pa/Th against the core top database as shown in (van Hulten et al., 2018) – see response to reviewer 1 comments and the revised caption of Fig. 1
- The zonally averaged dissolved and particulate Pa, Th and Pa/Th N-S Atlantic profiles (as shown on Figure 6 (Gu and Liu, 2017)) – Figure S1.
- The dissolved Pa and Th along GEOTRACES transect GA02 S using the data from (Deng et al., 2014) – please note that there are no particulate (only dissolved) data published in the latter article – Fig. S2
- The dissolved and particulate Pa and Th and Pa/Th along the GEOTRACES transect GA03 using the data from (Hayes et al., 2015a, 2015b) – Fig. S3

The model-data agreement of the water column particulate and dissolved activities is extensively described in the SOM.

Additionally, hypotheses are offered for why 13C response leads Pa/Th (possibly biology and/or air-sea exchange slows down 13C response), yet given the setup of the model, it would be a missed opportunity not to conduct a more detailed diagnosis of modeled causes for the lead-lag relationships among the various tracers. If the reasons can be pinned down, the paper can make a more robust conclusion, even if it is model-depending. Is it possible to plot the biological changes before and after a hosing experiment? How about changes in the air-sea exchange rate? Depending on the

results of those plots, the paper can then present a fuller picture of the changes during a hosing experiment.

We thank the reviewer for asking us to further investigate the lag between carbon isotopes and Pa/Th responses to a decrease in NADW formation. Indeed, the model set up allows us to look at the total biologic productivity (Calcium carbonate and particulate organic carbon) changes across the hosing. However, as shown on Figures 4 and 5, the carbon isotopes response has a strong spatial variability. Therefore, plotting the marine productivity anomaly between the control period and the hosing peak (year 550 to 600) – i.e. before and after the hosing as suggested by the reviewer – will not help investigating the cause of the delayed carbon response which happens around year 800 in the deep NW Atlantic.

In order to investigate the potential causes for the carbon isotopes lag, we have plotted time series of relative organic carbon production, aqueous pCO_2 and sea surface temperature averaged over the North Atlantic, where the lag between Pa/Th and carbon isotopes is the most pronounced. We see that, in line with the classical hosing response described in the literature, the freshwater addition in the North Atlantic causes a decrease of the SST and the organic carbon production as well as an increase of the aqueous pCO_2. However, all those changes reach their maximum around year 600 (or shortly before) of the simulation, i.e. about 200 years before the $\delta_{13}C$ response around year 800 (in the deep basin). This indicates that the air-sea exchanges and the biological productivity are not directly responsible for the time lag between the carbon isotopes response and the AMOC slowdown. Looking at a series of N-S Atlantic sections, we can see that the $\delta_{13}C$ anomaly builds up in the North Atlantic intermediate waters above 3000 m from year 400 to 750. The maximum of the anomaly is located between 1500 and 3500 m around 50°N and spreads in the deep Atlantic from year 750. Therefore, we argue that the lag between the carbon isotopes response relative to the Pa/Th is likely due to the time necessary to transport the anomaly on site, in particular in the deep ocean. While the Pa/Th directly depends on the AMOC capacity to transport Pa southwards, the carbon isotopes form in the intermediate ocean because of changes in air-sea exchange and accumulation of nutrients related to the decrease in NADW formation. Therefore, it seems to take more time for the carbon isotopes anomaly to reach the deeper ocean through water mass advection.

We have revised the discussion section and added Figure 6 to include those findings in the revised manuscript. This study highlights a complex response of the different proxies to a rather classic circulation perturbation. The relationship between the proxies and the ocean circulation surely needs further work to be fully understood. We hope that our manuscript now presents a fuller picture of the changes happening during a hosing experiment.

Additional smaller points for consideration:
In P1L25 This is confusing. Should it read “without an a priori guess”?

Yes, we have now corrected this sentence.

In P1L33-34 These are not global changes and should be more narrowly defined, possibly as regional or even local.

Done

In P1L36, it should be “see Lynch-Stieglitz (2017) for a review”.

Done

In P1L40, "Nd, Cd/Ca, sortable silt are also valuable proxies to reconstruct circulation and water mass and they are worth mentioning.

We have now changed the sentence by:

“To date, among the numerous tracers available (e.g. benthic $\delta^{18}O$, Nd isotopes, Cd/Ca or sortable silts), the sedimentary ($^{231}Pa_{xs,0}/^{230}Th_{xs,0}$) ratio (hereafter Pa/Th) and dissolved inorganic carbon isotopes ($\delta^{13}C$, $\Delta^{14}C$) are key tracers to reconstruct and quantify past circulation patterns and water mass flow rates.”

In P2L25, this should be 12C, although in truth it is both, with a lower 13C/13C.

We thank the reviewer for highlighting this typo. This has now been corrected.

In P4L17, Equation 2, the second minus sign is different from the first. The multiplication dot is positioned as a punctuation would.

This has now been corrected

In P4L34, Equation 4, the “d” in “Kd” should be subscript.

Done

In P5L14, it should be “compiled in Dutay et al. (2009)”.

This comment is no longer valid as we now evaluate the model performance using GEOTRACES dataset as requested by the two reviewers.

In P6L13, this is a long and potentially confusing sentence, yet a valuable one for its description of how the proxies were evaluated. It would help to have a comma after “identify”, which might make it clearer that the identification is of simulation periods exceeding a defined length, for each proxy.

We thank the reviewer for the suggestion that we adopted.

In P8L3-5, this is a bold statement that just does not ring true. Ten thousand years for equilibration of the carbon isotope signal in the Atlantic ocean, and a thousand for Pa/Th? This is in a basin where the residence time of the deep waters is a few hundred years today, and maybe a thousand years more in the past. Unless I misunderstand the point here, something is not right.

We thank the reviewer for his/her careful reading. However, we confirm that this is not a “bold wrong statement”. Indeed, because Pa and Th, on the one hand, and the carbon isotopes, on the other hand, undergo very different processes in the ocean water column, the simulation time required to equilibrate these different tracers is very different. For instance, carbon isotopes are exchanged between different reservoirs such as the atmosphere, the ocean, the terrestrial and marine biosphere while the Pa and Th stay in the oceanic compartment.

We indeed agree that the residence time of deep waters is about a few hundreds of years today and could have increased up to thousands of years in the past in the Atlantic basin. However, Pa and Th residence time in the water column is **not related** to the residence time of the deep-water masses. Instead, the residence time of Pa and Th in the water column depends on how fast these two isotopes are scavenged to the sediments by particles sinking in the water column. In other words, the **observed** residence time of Pa and Th in the water column remains up to **200 years for Pa** and **40 years for Th** (Henderson and Anderson, 2003), independently of the overturning circulation rate.

From the model side, (van Hulten et al., 2018) obtain negligible Pa and Th drifts, of less than 0.1% after 500 years of equilibration. Please find below the text from (van Hulten et al., 2018) on this topic :

“The model was spun up for 500 years, after which it was in an approximate steady state (decadal drift of −0.002 % for total ^{230}Th and +0.058 % for total ^{231}Pa). Protactinium-231 has a larger drift than thorium-230 because ^{230}Th is more quickly removed everywhere in the ocean because of its high particle reactivity. The lithogenic particles are in a steady state, and the PISCES variables are in an approximate steady state (e.g. phosphate shows a drift of −0.005 % per decade).”

The figure below shows the evolution of the global averages for dissolved and particulate Pa and Th after a fresh-start (all activities are initialized to 0). Therefore, we may consider that the Pa/Th tracer is at equilibrium after 1000 years of simulation.

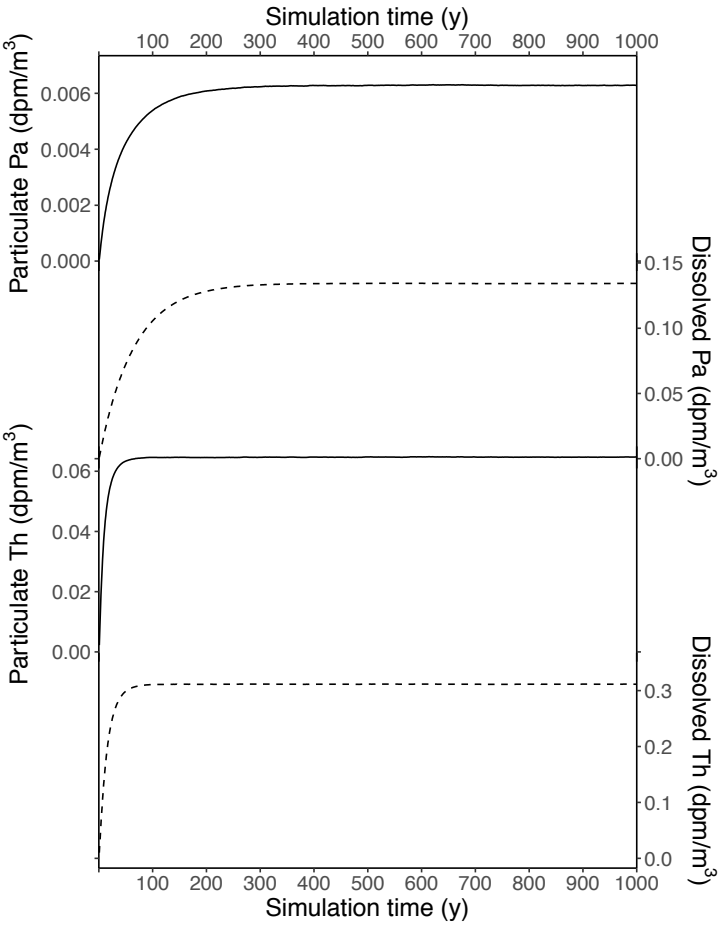

In P8L26, when listing the reasons that the millennial scale climate changes are not analogous to the hosing experiments, it would be useful to also point out that the location of the freshwater hosing in the model (the Nordic Seas) could also be different from events that originate primarily from the Laurentide ice sheet on North Americal, mostly likely including the millennial Dansgaard-Oeschger and Heinrich events.

We thank the reviewer for highlighting this point. We have changed the text accordingly:

"However, our hosing experiments are not direct analogues of the millennial scale climate changes of the last glacial cycle because i) glacial millennial events occurred under glacial conditions whereas our simulations were run under PI conditions, ii) the Heinrich and DO events have distinct proxy patterns and cannot be entirely explained by a simple fresh water addition in the North Atlantic and iii) the freshwater inputs might have occurred in different locations across distinct millennial scale events (e.g. originating from the Laurentide or Scandinavian ice sheet) while in the model, the freshwater was only added in the Nordic seas."

P9L10, substitute “If” with “While”.

Done

P9L32, modeled 13C results are compared with another model’s results, yet this section is named “Comparison to proxy data”. Maybe update section title to “Comparison to proxy and modeled data.”

We thank the reviewer for his suggestion that we have implemented.

In Figure 2, the labels (e.g. A. Single response) are unnecessarily far from the plots. The caption should define the dotted black lines (which I assume is the 2 sigma variation of the control phase). Also in the caption, the dotted red vertical line is the response time and the dotted red horizontal line is the proxy response. The caption states it the other way.

We thank the reviewer for highlighting these issues. Figure 2 and its caption have been edited accordingly.

In Figure 3, I think I’m missing something here. Why are there overlaps between the data coverage of single and dual response plots? Shouldn’t the two be mutually exclusive?

As pointed out by the reviewer, single and dual responses are clearly mutually exclusive. However, as explained in our response to reviewer 1, Figure 3 shows zonal averages for the western Atlantic N-S section. Consequently, for one grid cell to appear blank on Figure 3 A. (resp. 3.B.) it is required that the zonal average is empty and consequently that there is no grid cell in the full longitude range considered, displaying a single response (resp. dual response). Therefore, it is possible to have overlaps on Figure 3. We added a sentence to Figure 3’s caption in order to clarify this point.

Lastly, a citation in your references has the wrong publication year. The citation for “Luo, Y., Francois, R. and Allen, S. E.: Sediment 231Pa/230Th as a recorder of the rate of the Atlantic meridional overturning circulation: insights from a 2-D model., Ocean Science Discussions, 6(4), 2755–2829, 2009.” should instead be Luo, Y., Francois, R., and Allen, S. E.: Sediment 231Pa/230Th as a recorder of the rate of the Atlantic meridional overturning circulation: insights from a 2-D model, Ocean Sci., 6, 381-400 https://doi.org/10.5194/os-6-381-2010, 2010.

We thank the reviewer for highlighting this typo. This is now corrected.

References:

Deng, F., Thomas, A. L., Rijkenberg, M. J. A. and Henderson, G. M.: Controls on seawater 231Pa, 230Th and 232Th concentrations along the flow paths of deep waters in the Southwest Atlantic, Earth Planet. Sci. Lett., 390, 93–102, doi:10.1016/j.epsl.2013.12.038, 2014.
Gu, S. and Liu, Z.: 231 Pa and 230 Th in the ocean model of the Community Earth System Model (CESM1. 3)., Geosci. Model Dev., 10(12), 2017.
Hayes, C. T., Anderson, R. F., Fleisher, M. Q., Huang, K.-F., Robinson, L. F., Lu, Y., Cheng, H., Edwards, R. L. and Moran, S. B.: 230Th and 231Pa on GEOTRACES GA03, the U.S. GEOTRACES North Atlantic transect, and implications for modern and paleoceanographic chemical fluxes, Deep Sea Res. Part II Top. Stud. Oceanogr., 116, 29–41, doi:https://doi.org/10.1016/j.dsr2.2014.07.007, 2015a.
Hayes, C. T., Anderson, R. F., Fleisher, M. Q., Vivancos, S. M., Lam, P. J., Ohnemus, D. C., Huang, K.-F., Robinson, L. F., Lu, Y., Cheng, H., Edwards, R. L. and Moran, S. B.: Intensity of Th and Pa scavenging partitioned by particle chemistry in the North Atlantic Ocean, Mar. Chem., 170, 49–60, doi:https://doi.org/10.1016/j.marchem.2015.01.006, 2015b.
Henderson, G. M. and Anderson, R. F.: The U-series toolbox for paleoceanography, Rev. Mineral. Geochem., 52(1), 493–531, doi:10.2113/0520493, 2003.
van Hulten, M., Dutay, J. C. and Roy-Barman, M.: A global scavenging and circulation ocean model of thorium-230 and protactinium-231 with realistic particle dynamics (NEMO–ProThorP 0.1), Geosci Model Dev Discuss, 2017, 1–32, doi:10.5194/gmd-2017-274, 2018.
Rempfer, J., Stocker, T. F., Joos, F., Lippold, J. and Jaccard, S. L.: New insights into cycling of 231Pa and 230Th in the Atlantic Ocean, Earth Planet. Sci. Lett., 468, 27–37, doi:https://doi.org/10.1016/j.epsl.2017.03.027, 2017.
Schlitzer, R., Anderson, R. F., Dodas, E. M., Lohan, M., Geibert, W., Tagliabue, A., Bowie, A., Jeandel, C., Maldonado, M. T. and Landing, W. M.: The GEOTRACES intermediate data product 2017, Chem. Geol., 493, 210–223, 2018.